AD-A111 338

AD

AD-E400 756

CONTRACTOR REPORT ARLCD-CR-81054

REDUCTION OF SAFE SEPARATION DISTANCES FOR HAZARDOUS MATERIALS TRANSPORTED IN BUCKETS THROUGH RAMPS AT LAP PLANTS

F. E. SLATER
E. P. BERGMANN
SOUTHWEST RESEARCH INSTITUTE
6220 CULEBRA ROAD
SAN ANTONIO, TEXAS 78284

W. O. SEALS, PROJECT ENGINEER
R. M. RINDNER, PROJECT LEADER
ARRADCOM

DECEMBER 1981

US ARMY ARMAMENT RESEARCH AND DEVELOPMENT COMMAND
LARGE CALIBER
WEAPON SYSTEMS LABORATORY
DOVER, NEW JERSEY

APPROVED FOR PUBLIC RELEASE; DISTRIBUTION UNLIMITED.

UNCLASSIFIED

SECURITY CLASSIFICATION OF THIS PAGE (When Data Entered)

REPORT DOCUMENTATION PAGE

READ INSTRUCTIONS BEFORE COMPLETING FORM

1. REPORT NUMBER Contractor Report ARLCD-CR-81054	2. GOVT ACCESSION NO.	3. RECIPIENT'S CATALOG NUMBER
4. TITLE (and Subtitle) REDUCTION OF SAFE SEPARATION DISTANCES FOR HAZARDOUS MATERIALS TRANSPORTED IN BUCKETS THROUGH RAMPS AT LAP PLANTS		5. TYPE OF REPORT & PERIOD COVERED Final 6. PERFORMING ORG. REPORT NUMBER 02-6163-001
7. AUTHOR(s) F. E. Slater and E. P. Bergmann, SwRI W. O. Seals, Project Engineer, ARRADCOM R. M. Rindner, Project Leader, ARRADCOM		8. CONTRACT OR GRANT NUMBER(s) DAAK10-80-C-0166
9. PERFORMING ORGANIZATION NAME AND ADDRESS Southwest Research Institute 6220 Culebra Road San Antonio, Texas 78284		10. PROGRAM ELEMENT, PROJECT, TASK AREA & WORK UNIT NUMBERS MMT-5804288
11. CONTROLLING OFFICE NAME AND ADDRESS ARRADCOM, TSD STINFO Div (DRDAR-TSS) Dover, New Jersey 07801		12. REPORT DATE December 1981 13. NUMBER OF PAGES 88
14. MONITORING AGENCY NAME & ADDRESS(if different from Controlling Office) ARRADCOM, LCWSL Energetic Systems Process Div (DRDAR-LCM-SP) Dover, New Jersey 07801		15. SECURITY CLASS. (of this report) Unclassified 15a. DECLASSIFICATION/DOWNGRADING SCHEDULE

16. DISTRIBUTION STATEMENT (of this Report)

Approved for public release; distribution unlimited.

17. DISTRIBUTION STATEMENT (of the abstract entered in Block 20, if different from Report)

18. SUPPLEMENTARY NOTES

This project was accomplished as part of the U.S. Army's Manufacturing Methods and Technology Program. The primary objective of this program is to develop, on a timely basis, manufacturing processes, techniques, and equipment for use in production of Army materiel.

19. KEY WORDS (Continue on reverse side if necessary and identify by block number)

Safe separation	Aluminum containers	Transport buckets
Propagation	ABS containers	Ramps
Detonation	Plastic containers	Ramp coverings
Deflagration	MMT-Sensitivity	
Composition B	Conveyors	

20. ABSTRACT (Continue on reverse side if necessary and identify by block number)

The purpose of this program was to evaluate and select materials for ramps and transport buckets that could reduce safe separation distances for hazardous materials in transit between buildings. Several thicknesses of aluminum, types of plastics, and material configurations were evaluated as candidate items for use in manufacture of transport buckets. Ramp-covering materials of Styrofoam®, acoustic blanket material, and corrugated fiberglass were also compared.

It was determined that plastic materials offer a significant advantage over solid aluminum for buckets in the reduction of safe separation distances. (cont)

DD FORM 1 JAN 73 1473 EDITION OF 1 NOV 65 IS OBSOLETE

UNCLASSIFIED

SECURITY CLASSIFICATION OF THIS PAGE (When Data Entered)

20. ABSTRACT (cont)

However, a sandwich configuration consisting of an aluminum sheet, an aluminum honeycomb, and another aluminum sheet forms a rigid bucket which provides a safe separation distance approaching that provided by a plastic bucket.

It was determined that the ramp-covering material influences the safe separation distances as a function of its area density. This influence, however, is a second-order effect compared with the pressure intensity. If the area density of the ramp-covering material is below 0.8 kg/m^2, the selection of the covering can be based on cost and utility factors without a deleterious effect on the safe separation distance.

A safe separation model was formulated and, although incomplete, provides a first-order basis for estimating safe separation distances.

CONTENTS

TABLES

FIGURES

INTRODUCTION

This report describes a series of full-scale test evaluations which was conducted in support of the U. S. Army Plant Modernization Program. These evaluations were oriented toward those activities within various Army Ammunition Plants that require the conveyance of bulk explosives/ propellants in transport buckets through ramps. The evaluations were conducted under the guidance of the Energetic Systems Process Division, U. S. Army Research and Development Command, Dover, New Jersey.

Optimization of plant layouts and production efficiencies can be attained when the distances between hazardous materials on a conveyance system can be minimized. Current plant configurations do not generally permit utilization of optimum minimum distances because of the fragmentation environment generated by conveyor systems and transport buckets. Separation distances are further increased because the ramps through which the conveyor systems operate tend to confine and focus the blast and fragment effects.

The objectives of the test series were to design and evaluate ramps and transport buckets using commercially available construction materials that could substantially reduce the safe separation distances between hazardous materials in transit, within ramps between buildings at Army Ammunition Plants.

The succeeding sections of this report detail pre-test evaluations, test procedures, results achieved, analysis of data in the formulation of a safe separation model, conclusions drawn, and recommendations.

DISCUSSION OF PRE-TEST EVALUATIONS

Relevant Considerations

Prior to the commencement of safe separation testing, certain relevant considerations pertaining to the characteristics of the materials used in ramp and transport bucket construction were reviewed. Ramp characteristics influence the safe separation distance in two ways: the pressure can be reflected from the floor, walls, and roof, in such a way that it reinforces the primary pressure pulse emitted by the donor; and fragments from the donor can ricochet from the ramp walls and ceilings and be directed toward the acceptor. The reflection of the donor's pressure pulse is a function of the shape of the ramp, and the mass per unit area, area density, or the material making up the ramp walls and roof. Material strength has little influence unless that strength is low enough to allow the material to disintegrate as the pressure pulse strikes. The trend, then, has been to make the ramp covering from light material, like aluminum or fiberglass, and to use shape effects, such as corrugation, to provide the necessary rigidity to take the environmental loads.

There have been few studies on ways to mitigate reflected shock pressures. However, there appear to be at least two ways in which the intensity of the reflected pressure can be mitigated. They are:

1) Use of lightweight tunnel materials. The effects of explosions can be mitigated, and at times controlled, through the use of blow-out panels. These panels provide pressure relief for a closed system

if the inertia of the panel is low and the panel area is high. A pressure wave from a detonation of an explosive has much higher pressures and pressure rise rates than is experienced in an explosion. The pressure relief from blow-out panels, then, is not practical in a detonation environment. However, to minimize the inertial resistance of the tunnel material, the area density must be minimized.

2) Use of energy absorbing tunnel materials. The more shock energy that can be absorbed, the less is available for reflection. There are at least two ways to absorb the energy: through internal deflection and through offering a low resistance to the pressure pulse as it passes through the material. Sound is absorbed by providing internal spaces in which the sound wave can get trapped. It is also absorbed by allowing the sound to reflect from surfaces in such a manner that the reflected waves interact to reduce the reflected energy. Both principles were applicable in the selection of a suitable tunnel material.

A third alternative is to alter the ramp configuration in such a way that the pressure wave reflections are not directed down the ramp. This would be feasible only if the explosive charges had specific locations within the ramp (e.g., not on a conveyor).

There were four requirements related to transport bucket materials. They include:

1) The bucket material must be compatible with in-plant materials handling systems.

2) When the explosive in the donor bucket is initiated, the donor

bucket material should fragment in such a way that the fragments have a low average mass.

3) The acceptor bucket material should have the strength to resist successfully the impact of fragments from the donor bucket.

4) The bucket configuration should be such that a minimum number of fragments are directed down the tunnel.

In a previous program[1] it was found that in-plant materials handling loads require a relatively rigid transport bucket configuration. Since it is desirable to have a long bucket life, the material must have good wear characteristics. Aluminum and stainless steel material have been used as bucket materials[1,2]. In a visit to a grain elevator by SwRI staff members, it was learned that the transport buckets used in the elevator were made of plastic. Previously the buckets had been made from stainless steel, but the plastic material provided a stronger, lighter bucket that had three times the wear life of the steel buckets.

When explosives are initiated in the donor, three fragment properties are important in the determination of the safe separation distance: 1) average fragment mass, 2) average fragment velocity, and 3) fragment density. The expected fragment mass distribution can be estimated from the formulas of Mott and Linfoot[3]. The equations are of the form:

$$N(m) = N_o e^{-(m/\mu)^a} \tag{1}$$

where: $N(m)$ = number of fragments of mass greater than (m)

N_o = total number of fragments $(m/2\mu)$

2μ = arithmetic average fragment mass

m = total mass of warhead case

a = constant (a = 1/2 for two-dimensional breakup;

a = 1/3 for three-dimensional breakup)

The Gurney-Sarmdusakis formula[3] for the average fragment mass is of the form:

$$\mu^{1/2} = \frac{At\,(di + t)^{3/2}}{di}\sqrt{1 + \frac{1}{2}\left(\frac{c}{m}\right)} \tag{2}$$

where: A = constant relating to explosive composition

t = casing thickness

di = diameter of warhead

c/m = charge-to-metal mass ratio

The scaling constant, A, varies from a value of 1.01 for cyclotol to 2.55 for baratol. For Composition B the value is 1.14.

Experiments show that some materials exhibit smaller fragments than others. For instance, forged or cast steel produces larger mass fragments than do malleable or ductile cast irons. However, no correlation was found between fragmentation and strength or between fragmentation and ductility of the casing material[3].

The fragment velocity is usually determined by the Gurney formulas[3] which are of the form:

$$V_o = D\,\frac{c/m}{\sqrt{1 + b(c/m)}} \tag{3}$$

where: V_o = initial fragment velocity

D = the Gurney constant which is explosive material dependent

b = a shape factor (b = 0.5 for cylinders; 0.6 for spheres)

Examination of equations 1, 2, and 3 shows that material properties, other than mass, do not appear in the equations. This may be due, in part, because the equations were derived from warhead test data and most of the warheads are steel or cast iron.

In a recent program for ARRADCOM[1] it was found that the c/m ratio has an influence on safe separation. In general, for metal transport buckets, the higher the c/m, the greater the safe separation distance. This relationship, however, did not hold for very weak containers, such as cardboard. This in turn implies that there is a material property effect that should be considered.

Equation 1 indicates that the fragment size can be controlled to some extent by making the walls of the buckets as thin as possible. Experiments on safe separation[1] also showed that thin-walled buckets reduced the safe separation distance. The problem comes in the loss of bucket rigidity through the use of thin walls.

If we reverse our viewpoint and examine the acceptor, it is evident that the transport bucket material should resist the high shock pressures of the blast wave and have the strength to mitigate the impact effects of the donor fragments. Kevlar armor was used to shield the acceptor[1,2] and thereby reduce the safe separation distance from that established without armor. The kevlar was an ideal material in that it disintegrated into fine particles when hit by a shock wave and it was tough enough to withstand fragment impacts. A plastic bucket material could provide the same virtues if it can be shown to be compatible with the handling system. A honeycomb material between thin-walled aluminum should be practical also because tests with thin-walled buckets[1] were successful.

Bucket configurations can also be used to an advantage. If the donor and acceptor buckets were square and their faces parallel (□ □) the impact angle of obliquity provides the most unfavorable impact conditions as well as the maximum number of impacting fragments. If, however, the donor and the acceptor faces are each rotated 45° (◇ ◇) the primary donor fragment direction is away from the acceptor and the threat to the acceptor is primarily from ricochet impacts. Also, the effective thickness of the acceptor skin is increased by about 40%. Cylindrical buckets (○ ○) would also reduce the area of major direct fragment impact.

Site Visitations

After a careful review of the aforementioned considerations, it was deemed necessary that visitations be made to several in-plant operations to obtain the ramp and bucket designs currently used in the transportation of materials through ramps. Additionally, information was required to facilitate the next phase of the program, materials search. Relevant data required included:

1. Type construction material in the ramps

2. Present safe separation distances

3. Type of materials transported

4. Configuration and material used in the construction of current transport buckets

5. Constraints (such as deflections, allowable sizes, configurations, impact and rough handling considerations) which needed to be determined in order to establish the bounds of bucket designs

6. Conveyor interface and conveyor configurations

7. Production rates and the influence that safe separation distances play in productivity

Plant Visits

SwRI personnel visited two Army Ammunition Plants: Lone Star AAP, Texarkana, Texas, and Louisiana AAP, Shreveport, Louisiana.

At each plant, it was noted that the primary material used in the construction of transport buckets was 6061-T6 aluminum. At the new melt/pour facility at Lone Star AAP a large fiberglass bucket coated with a conductive material was used to transport Composition B. Bucket designs were cylindrical (Figure 1) and square (Figure 2) and varied in thickness. The principle means of conveyance was provided by overhead conveyors (Figure 3). Rail-type conveyors and steel roller conveyors were utilized in some operations.

The quantity of explosives being transported ranged in weight from 11.3 kg to 29.9 kg and the types of explosives being moved consisted of TNT, Composition A-5, Composition B, and Composition C-4. The separation distance between transport buckets carrying 11.3 kg of explosive, regardless of type, was 9.2 meters. Operating lines conveying larger quantities of explosives were not in operation during the visit and separation distances were not made available.

Conferences with the personnel at each plant visited revealed the primary considerations in the selection of alternate materials for transport buckets must be conductivity and durability. Further discussion revealed that most conveyor systems were capable of being operated at various speeds and to date separation distances did not adversely affect production rates or efficiencies.

The site visitations revealed that ramp construction was not uniform. Ramp configurations varied from wooden frame construction to steel construction, utilizing I-beams, channel and/or angle iron (Figure 4). The walls of the ramps were sheathed with corrugated fiberglass, wood siding, metal siding (which ran the gamit of corrugated steel), V-beam aluminum, and an insulated steel siding. One consistent factor noted in the construction of the ramps was the fact that all the roofs were of corrugated steel or wood decking covered with asphalt sheeting.

During visitations, it was noted that on some operating lines the aluminum transport buckets were surrounded by steel strappings which were generally 6.4 mm thick by 25.4 mm to 76.2 mm wide (Figure 5). This condition would affect adversely any reduction of safe separation distances gained by judicious selection of bucket materials.

Materials Search

Several considerations were necessary in the search for alternate ramp and transport bucket construction materials. Ramp materials needed to be energy absorbing through internal deflection and by offering a low resistance to the pressure pulse as it passes through the material. The material must also maintain the capabilities to withstand environmental and climatic conditions.

A careful review of these considerations led to the selection of Styrofoam® and an acoustical blanket material of spun fiberglass.

These materials ideally meet the requirements of the necessary energy absorbing features noted above and can be made to meet the requirements of environmental and climatic conditions.

Styrofoam and spun fiberglass are used in the manufacture of many industrial products requiring strength and durability. Perhaps the most revealing example is the construction of water craft. Enhancement of resistance to climatic conditions may be accomplished through utilization of special coatings.

In the case of materials for the construction of transport buckets, requirements considered were: 1) conductivity of the material, 2) compatibility of the material with the explosives being transported, and 3) ruggedness of the materials to withstand the extremes of daily use and rough handling.

Two basic materials fell well within the purview of these requirements: metals and thermoplastics. Previous test programs[1,2,4] had shown that the use of metallic materials required distances that were, in some cases, considered excessive in that they adversely affected productivity in plant operations. The use of thin metals[1] did indicate that sufficient reductions in safe separation distances could be achieved. However, thinner walled transport buckets were not consistent with long service life or rough handling. With this in mind, thin aluminum, 1.6 mm thick, used to sandwich an aluminum or a nonmetallic honeycomb material would provide the strength and rigidness needed to meet the service life requirement.

Consideration was given to the utilization of powdered metals. These were discarded when it was learned from the industry that powder metals, when compressed under heat and pressure, have approximately 96% of the density of rolled metals and would produce a fragmentation environment equivalent to the metal materials currently being used and that current technology can only form very small components of powder metals.

The use of aluminum or nonmetallic honeycomb showed promise in that such material when sandwiched between thin aluminum would act as a shock absorbent to the loads presented as a result of a detonation. Nonmetallic honeycomb materials were eliminated primarily because some concern was directed at the possibility of creating a large capacitor effect within the transport bucket.

As a result of this survey and the careful scrutiny of all the considerations previously stated, two aluminum honeycomb materials were selected for preliminary testing: 3.2 mm honeycomb, 12.7 mm thick, and 9.5 mm honeycomb, 12.7 mm thick, each sandwiched between two pieces of 1.6 mm thick 6061-T6 aluminum plate (Figure 6).

The consideration of thermoplastics for use as transport buckets provided some problem areas not associated with metals. These areas of concern were conductivity, compatibility with the wide variety of plastic materials available, and the commercial market. Discussion with representatives of manufacturers of plastic resins showed that conductivity can easily be attained by the introduction of carbon black, 10 to 20% by weight, or the introduction of carbon fibers to the resin.

Compatibility with the materials being transported was attained by selecting from a list of materials which are compatible with Composition B, Cyclotol, and TNT, as provided by ARRADCOM.

After careful consideration, four candidates were selected for preliminary testing:

- Acrylonitrile Butadiene Styrene (ABS)
- Polypropylene
- Polycarbonate
- Polyphenylene Sulfide

These materials were selected on the physical characteristics of each as shown in Table 1.

DISCUSSION OF TEST PROCEDURES AND EVALUATION OF RESULTS

Tests were conducted in four phases, each phase designed to establish the merits of the materials to be tested and to confirm the results. The testing program was broken down as follows:

- Phase I. Arena tests were conducted to accumulate data relative to fragment size, fragment mass, penetration data, impact velocities, and resistance to shock and fragment impacts.
- Phase II. Safe separation tests in open air to establish minimum distances for the materials selected in Phase I.
- Phase III. Ramp tests to evaluate the physical properties of the materials selected for the ramp walls. This evaluation included the ability of the materials to mitigate the focus of reflected waves down the ramp. This phase included the confirmation of a safe separation distance in the ramp utilizing the material selected.
- Phase IV. Amass and analyze the accumulated date and establish a safe separation model.

Arena Tests

Having made the selection of materials deemed of the right type for the construction of transport buckets, a requirement existed to determine which of these materials would be best suited for use in actual operations. The data required for this determination were fragment size, mass, penetration ability, and the resistivity of the material to defeat fragment impacts generated by the detonation of a donor bucket.

To collect these data, a series of arena tests was conducted in which a donor bucket containing 30.9 kg of Composition B was placed in an arena of Cellotex (Figure 7). Each bucket was constructed rectangular in shape (Figure 6) and measured 355.6 mm wide by 457.4 mm long by 203.2 mm high. The thickness was dependent on the material being tested. The thickness is as follows:

Thermoplastics: ABS, Polycarbonate, Polypropylene, and Polyphenylene Sulfide...6.4 mm

Metals, 6061-T6 Aluminum...3.2 mm thick and 1.6 mm thick

Honeycomb...12.7 mm thick.

Cellotex panels were placed 4.6 meters from the donor charge and each panel was 406 mm thick, 1.22 meters high by 2.44 meters long. On one panel a like piece of the material being tested was placed as a witness panel to ascertain the resistivity to fragment impact (Figure 8). The donor bucket was initiated by a booster charge of 114 grams of Composition C-4 placed in the bottom of the bucket and primed with a M-6 Electric Blasting Cap.

Of the metal materials tested, the 3.2 mm 6061-T6 aluminum indicated the most severe environment and was representative of the buckets previously evaluated(1). Figure 9 illustrates the severity of the fragment impacts and provided a baseline for comparison. Utilization of this material required safe separation distances of 9.1 meters with 27.3 kg of Cyclotol.

Table 2 outlines the quantity of penetrations received by the various witness panels and the depth of penetration into the Cellotex panels. Figures 10 through 15 depict the variance in fragment hits versus fragment penetrations. Fragments from each material were extracted from the wallboard panels. Fragment and penetration data for the eight materials are given in Table 3. The layers of wallboard penetrated--as well as the fragment size, fragment mass, and number of fragments extracted from each wallboard layer --are shown. An inspection of the table indicates:

- ABS fragments penetrated only 25 mm of wallboard. This represents the lowest maximum penetration for the samples of plastic materials evaluated.

- The 9.5 mm aluminum honeycomb, 12.7 mm thick, faced with 1.6 mm 6061-T6 aluminum sheets also penetrated only 25 mm of wallboard. This represents the lowest maximum penetration for the samples of aluminum materials evaluated.

- The 3 mm thick aluminum panels produced fragments that penetrated 114 mm of wallboard.

To calibrate the wallboard in terms of fragment velocity, fragment size and penetration characteristics, a test series was conducted in which lead projectiles were fired against the wallboard. Projectile size, mass, velocity and penetration were recorded. Based on these tests, it is postulated that the penetration can be expressed by:

$$\frac{P}{\bar{L}} = 0.00000839 \frac{\rho_T \dot{X}_o^2}{\rho_P^2} - 3.6 \qquad (4)$$

where: P = penetration depth, mm

$\bar{L}$ = characteristic fragment diameter, mm

$\dot{X}_o$ = fragment impact velocity, m/sec

ρ_T = target density, gm/mm^3

ρ_P = fragment density, gm/mm^3

For wallboard, the target density is 0.000246 gm/mm^3. If this value is substituted into equation 4, the fragment velocity can be estimated from:

$$\dot{X}_o = \left(\left(\frac{P}{\bar{L}} - 3.6\right)\left(\frac{\rho_P^2}{2.064 \times 10^{-9}}\right)\right)^{1/2} \tag{5}$$

$\bar{L}$ is estimated to be:

$$\bar{L} = \frac{W + T}{2} \tag{6}$$

where: $\bar{L}$ = characteristic fragment diameter, mm

W = average fragment width, mm

T = average fragment thickness, mm

Table 4 is a compilation of the estimated fragment impact energies and velocities for the materials, fragments and penetrations observed. The results are presented graphically in Figures 16 and 17. Figure 16 shows the fragment velocity relation. The solid data points are from the plastic materials and the open data points are from the aluminum materials. The penetration-velocity relation predicted appears to provide a reasonable model for the plastic materials. The scatter is more significant for the aluminum panels. The graph indicates that the plastic panels produce fragments of lower velocities than are produced from the aluminum panels.

Figure 17 shows the penetration-fragment kinetic energy relationship. The fragment kinetic energy-penetration relationship appears to have somewhat less scatter than does the penetration-velocity relationship. The plastic materials, as a rule, produce fragments with lower kinetic energy and less penetration than do the aluminum panels. Clearly, the plastic material shows improved safe separation potential over the aluminum material if the cost, materials handling, durability and safety can be shown to be acceptable.

On the basis of the data accumulated in the arena testing, two materials, one aluminum and one plastic, were selected for full-scale safe separation testing. These materials were:

- Acrylonitrile Butadiene Styrene (ABS)
- 9.5 mm aluminum honeycomb, 12.7 mm thick sandwiched between two sheets of 1.6 mm thick 6061-T6 aluminum.

The polycarbonate was eliminated as a candidate for testing based on the cost of this material versus Acrylonitrile Butadiene Styrene. The polypropylene and polyphenylene sulfide (Ryton) were rejected due to the fragmenting of the witness panels from blast pressures during the arena testing. These materials were considered too brittle and less conducive to the rigors of normal day-to-day use.

Phase II-Safe Separation Tests in Open Air

Based upon the data accumulated in the arena tests, a series of open-air tests was conducted using transport buckets constructed of acrylonitrile butadiene styrene 6.4 mm thick, and aluminum transport buckets. The ABS transport buckets, donor and acceptors, were 356 mm wide by 457 mm long by 203 mm high. These containers were fabricated locally using an adhesive of ABS resin and methylene chloride. The aluminum transport buckets were configured with a 9.5 mm core aluminum honeycomb sandwiched between two panels of 1.6 mm thick 6061-T6 aluminum (Figure 18).

In each of the open-air tests, a donor bucket was placed in the center of an area with one acceptor placed at 90°, 180°, 270°, and 360° from the donor. The distance at which the acceptors were placed from the donor was predicated on the results of the initial test to be described below. The donor and acceptor transport buckets each contained 30.9 kg of Composition B and each was situated 0.76 meters off the surface of the ground by pedestals of Sonotube®*. The donor was initiated by a M6 Electric Blasting Cap in a 114 gram booster charge of Composition C-4 located in the bottom of each donor bucket.

The first test in the open-air series was an effort to identify quickly at what distance would propagation by detonation occur or not occur. To make this assessment, the four acceptors were placed at four different distances from the donor. These distances, measured edge-to-edge from the donor, were 2.4 meters, 3.6 meters, 4.9 meters and 6.1 meters (Figure 19). In this test, the donor and acceptors were constructed of ABS. The acceptor situated at 2.4 meters propagated by detonation. The other three acceptors received fragment impacts but no fragments penetrated the walls of the acceptors at these distances. In this test, as with each test conducted in the program, the acceptor buckets came apart and the contents was scattered on the ground.

---

*Registered trademark of Sonaco Products Inc.

Based upon the observations made and the results of the above test, a series of open-air tests was carried out utilizing ABS transport buckets. As in the preliminary testing, a donor and four acceptors were used in each test, with each acceptor placed 3.6 meters, edge-to-edge from the donor. As noted in Table 5, no propagations by detonation or deflagration occurred. In each case, the walls of the acceptor buckets facing the donor were subjected to many fragment hits but no penetration of the bucket walls was noted. Figure 20 illustrates the typical damage sustained by the acceptor transport buckets. Figure 21 depicts the severity of damage sustained by some acceptors during this phase of testing. The cracking and fracturing of the ABS panels is primarily the results of blast wave pressures rather than fragment impacts.

Next, tests involving 6061-T6 aluminum honeycomb core were begun. Since 3.6 meters was considered the optimum safe separation distance utilizing ABS, two aluminum acceptor buckets were placed at this distance from the donor bucket. However, based on previous tests (Ref. 1) the fragmentation environment with these aluminum buckets would be more severe thus increasing the probability of propagation. For this reason, two of the acceptors were situated 4.9 meters from the donor. The results of this series of tests are shown in Table 6. Figure 22 shows the fragmentation penetrations of both the front and rear panels of the acceptor bucket at 3.6 meters while Figure 23 shows only penetration of the front panel at 4.9 meters.

On each open-air test involving both ABS and aluminum transport buckets, pressure measurements were taken using LC-33 pressure transducers.

Each transducer was suspended 0.76 meters above the ground and placed at 4.6 meters, 7.6 meters and 10.7 meters from the donor charge (Figure 24). The pressure data accumulated during these tests serves as a baseline for future comparisons with pressure measurements taken during the ramp tests.

Average pressures generated in the open-air testing were 574 kPa at 4.6 meters, 471 kPa at 7.6 meters, and 183 kPa at 10.7 meters. Time of arrival of blast wave pressure from transducer No. 1 (4.6 meters) to transducer No. 2 (7.6 meters) was 4.5 milliseconds while time of arrival between transducer No. 1 to transducer No. 3 was 9.7 milliseconds. The instrumentation used in these tests consisted of a four-channel biomation with a Tektronic type 602 display unit. Each LC-33 utilized an in-line conditioner model no. 402M71 and 402M72 and each signal passed through a Tektronic Model 483M37 PCB amplifier. The time signal was provided by a function generator. Table 7 outlines the settings used in these tests. Figure 25 shows the peak side-on pressures measured versus the scaled distance to the gauge.

Since no propagations of any type were noted during this phase of testing, 3.6 meters was considered the starting point for the safe separation distance in the next phase of the testing program, ramp tests.

Phase III-Safe Separation Tests in Ramps

Using a 3.6 meter separation, edge-to-edge between donor and acceptors, a series of full-scale tests was conducted to evaluate the physical properties and mitigating effects of Styrofoam and spun fiberglass (acoustic blanket) in a detonation environment. To evaluate these properties and their ability to mitigate effectively reflected shock pressures, pressure measurements were taken during the testing of each type of material. The relevance of the data accumulated from the measurements taken will be discussed later in this report.

Each test was conducted in a ramp constructed of 31.8 mm x 31.8 mm x 3.2 mm angle iron, sheathed with the material called for by the specific test, and each ramp measured 2.4 meters square x 9.6 meters long. All the tests, preliminary and confirmatory, utilized ABS transport buckets; one donor and two acceptors. As in the open-air tests, each transport bucket contained 30.9 kg of Composition B and each was placed on a Sonotube pedestal 0.76 meters above the ground. The donor was initiated by an M6 electric blasting cap in a 114 gram booster of Composition C-4 located in the bottom of the transport bucket. Figure 26 illustrates a typical test arrangement including the location of the pressure transducers.

Styrofoam and spun fiberglass (acoustic blankets) were of primary interest during this phase of the program. Two tests were carried out using corrugated fiberglass panels for the walls of the ramp. Fiberglass is used currently in plant construction. These tests provided a baseline source of data for comparison with the data to be amassed during future tests using Styrofoam and/or spun fiberglass (acoustic blanket).

Pressure measurements were taken by three LC-33 pressure transducers located at one end of the ramp. Each transducer was situated at 0.76 meters above the ground and positioned at 4.6 meters, 7.6 meters and 10.7 meters, respectively, from the donor bucket. As in the open-air tests, the instrumentation used in these tests consisted of a four-channel biomation with a Tektronic display unit, type 602. Each LC-33 used an in-line conditioner, PCB model No. 402M71 and 402M72 and each signal passed through a Tektronic amplifier Model 483M37. The time signal was provided by a function generator.

Table 8 shows the pressures derived for each material utilized for the ramp walls and those pressures generated in the open-air tests.

Regardless of materials utilized in the walls of the ramps, no propagations by detonation or deflagration(burning) were noted at a 3.6 meter separation during this phase of testing. In each case, the ramp was totally destroyed (Figure 27) and the contents of the acceptor transport buckets were strewn on the ground (Figure 28). The ABS transport buckets used as acceptors separated at their seams and the panels facing the donor bucket sustained damage from fragment impacts and blast pressures. Fragment impacts were characterized by dimpling the face of the panel (Figure 29) while, in some instances, severe fracturing of the panel took place as a result of blast pressures (Figure 30). The residual Composition B from each acceptor bucket showed signs of being subjected to high temperatures. Analysis of the 16 mm motion pictures taken during the testing depicted each acceptor being engulfed by the fireball generated by the detonation of the donor bucket.

The findings of these tests and the open-air tests provide sufficient evidence that 3.6 meters, utilizing ABS transport buckets, is the safe separation distance between transport buckets. Since propagation occurred at 2.4 meters in open-air and no propagation took place in any tests with the acceptors at 3.6 meters, the question arose: is 3.6 meters the minimum safe separation distance? In an endeavor to answer this question, one acceptor bucket was placed 3.0 meters from the donor in the final test in the series. Propagation by detonation occurred at this distance. Table 9 shows the results of the tests conducted during this phase of the program.

PREDICTION OF SAFE SEPARATION

In a previous safe separation program[1], it was shown that the probability of no propagations, burns or detonations, could be cast into a predictive equation. Indeed, it was indicated that a probabilistic predictive model could be developed, if enough experimental effort was committed. That program also indicated that the characteristic scaled distances for 100% no propagation (X_{100}) and 0% no propagation (X_0) could be predicted for some conditions of confinement. In this program, we have extended the predictive relationships developed by Bergmann[1] to include the conditions, materials and explosive of this program. We have also included data generated by Seals, et al.[4]. We have, however, recognized that the primary relationship of interest is X_{100}, the scaled distance for 100% no propagation, since that represents the safe separation distance. Also, it is apparent that the characterization of X_{100} only represents a significantly smaller effort than the development of the full model, since only one of the three relationships needs to be characterized. In this section of the report we will describe the data base used for the X_{100} model, the parameters of the model, alternate relationships developed and the usefulness and limits of the predictive relationships.

In the development of a safe separation predictive equation we would expect the following parameters to be important:

- Explosive energy
- Bucket mass and thickness

- Fragment energy, density, diameter, and length
- Bucket material toughness

In reviewing the data available from past safe separation programs, much of the requisite data have not been developed, or recorded. Also, material toughness data are not generally available for most of the bucket materials evaluated, and where such data can be found, they are based on slow strain rate tests. Therefore, based on the type of data generally available from handbooks, the following predictive relationship was postulated:

$$X_{100} = a + \left(\frac{c}{m}\right)^{b} \left(\frac{\rho_F tE}{\sigma_u^2}\right)^{e} \tag{7}$$

where:

X_{100}	=	scaled safe separation distance
c	=	explosive mass
m	=	bucket mass
ρ_F	=	bucket material density
t	=	bucket thickness
E	=	elastic modulus of bucket material
σ_u	=	ultimate strength of bucket material
a, b, e	=	constants

For most metals, the elastic modulus in flexure and tension is approximately equal as is the ultimate strength in flexure and tension. In plastics, however, there are significant differences. We found that the use of the flexural modulus and strength provides a more accurate prediction than does the use of the tensile values. Table 10 provides a summary of the safe separation model data base used to develop the predictive relationship. It is noted that the handbook data are used in English units, which is an accepted practice. Based on these data, the following predictive relationship is postulated:

$$X_{100} = 1.59 \times 10^{9} \left(\frac{c}{m}\right)^{9/4} \left(\frac{\rho_F t E_F}{\sigma_{u_F}^2}\right)^{5/2} \tag{8}$$

where: X_{100} = scaled safe separation distance, m/kg$^{1/3}$

c = TNT equivalent of explosive mass, kg

m = mass of the bucket, kg

ρ_F = bucket material density, lb/in.^{3}

t = bucket thickness, in.

E_F = Flexural modulus of elasticity of bucket material, lb/in.^{2}

σ_{uf} = flexural ultimate strength of bucket material, lb/in.^{2}

The deviation of the data from the prediction model of equation 8 is shown in Figure 31. Measured values of X_{100} are plotted against predicted values. The line of the figure represents a perfect fit locus. Predictions for the steel, aluminum and ABS containers are very close to the line. Predictions for the honeycomb and stainless steel containers are off of the line, but reasonably close. As an approximation, equation 8 is a reasonable first order prediction tool for safe separation.

During the development of equation 8 we recognized that the fit depended strongly on the material properties. This indicates that any further work in the development of a safe separation predictive equation should include the accurate measurement of the material properties of the containers. The effect of high strain rates on these properties should also be of interest.

It is to be noted that no prediction for the cardboard container was made due to the lack of material properties. We recognized that the protection of armor against projectile penetration is grossly dependent on the area density of the armor. On this basis, we cast the predictive relation for X_{100} into a form that replaces the second term of equation 2 by a density term. That form is:

$$X_{100} = 3.56 \times 10^{-8} \left(\frac{c}{m}\right)^{9/4} \left(\frac{\rho_F t}{\rho_o'}\right)^{5/2} \tag{9}$$

where: ρ'_o = air density (0.0000442766 $lb/in.^3/in.$)

The fit of equation 9 is shown in Figure 32. From this figure it is seen that the density dependent scaled safe separation distance prediction is a useful tool if limited material data are available. The prediction for the steel and aluminum containers is very reasonable; that for the cardboard container is also good; and that for the stainless steel container has not been hindered by the approximation postulated. Predictions for the honeycomb and ABS containers have been degraded somewhat, probably because the energy absorption capacity of these materials becomes a stronger influence.

Influence of Ramp Covering Material on Peak Side-on Pressure

Intuitively, it would be expected that ramps should be covered with as light a material as is practical to minimize the reflected shock strength, and thereby minimize the increase in safe separation distance over that established without ramps. This tendency was verified and grossly quantified in this program. Peak side-on pressure data for ramps covered with Styrofoam, acoustic blanket, and corrugated fiberglass were compared with pressure data from open-air tests. The results were cast into a predictive relationship which grossly characterizes the test results.

Table 8 is a compilation of the peak side-on pressure measured for each ramp material evaluated at three distances from the donor. The data are illustrated graphically in Figure 25. The dashed line represents the predicted open-air pressure-distance relationships to show the general trend expected. The measured data are grouped to the right of the predicted curve, and show significant scatter at the close scaled distance. The scatter decreases significantly as the distance is increased. At the close distances the magnitude of the peak pressure appears to be a strong function of the position of the gauge within the tunnel and its proximity of other items within the tunnel which influence the shock pattern. The scatter at the close standoff distances contributes materially to the scatter of the propagation results as the separation distance is decreased. This scatter would continue until the low pressure end of the scatter exceeds the critical propagation pressure. At that point, total propagation is reached.

The scatter of the data, particularly the close-in pressure data, tends to discourage the postulation of a predictive model based on this limited test series. It is desirable, however, to have a starting point for a predictive tool, which can be used to direct attention to the relative importance of the ramp covering material to the peak pressure. To that end, then, we postulate the following scaled side-on pressure relationship.

$$\frac{p_{s_o}}{p_o} = f\left(\frac{\rho_m'}{\rho_o A_s'}\right)^g \left[\left(\frac{c}{m}\right)^{1/3} \frac{\psi}{R}\right]^h \tag{10}$$

where: P_{so} = peak side-on pressure

P_o = ambient static pressure

ρ'_m = area density of ramp cover material (weight per unit area)

ρ_o = air density

A'_s = specific area of ramp cover (area per unit of length)

c = explosive mass

m = container mass

ψ = specific energy of explosive

R = separation distance

For this test series the following parameters were constant; P_o, ρ_o, A'_s , c, m, and ψ. Those parameters can be included in the constant, f′. Equation 10 then takes the form:

$$p_{s_o} = f'\left(\frac{\rho_m'}{\rho_o}\right)^g (R)^h \tag{11}$$

where ρ_o was left in the equation to allow ρ'_m/ρ_o to go to 1.0 for open-air conditions.

If we fit the data of Table 8 to the format of equation 11, the relationship that is developed is of the form:

$$p_{s_o} = 102{,}786\left(\frac{\rho_m'}{\rho_o}\right)^{.075} (R)^{-2.5} \tag{12}$$

Figure 33 shows the peak side-on pressure plotted against the ramp material area density ratio.

CONCLUSIONS

1. Safe separation distances currently in use at Army Ammunition Plants (AAP) can be reduced substantially by substituting thermoplastic transport buckets for the aluminum transport buckets.

2. Acrylonitrile Butadiene Styrene (ABS) supplies the most favorable characteristics of the materials evaluated.

3. For handling considerations and for fragment impact resistance ABS buckets should be at least 6.4 mm thick.

4. Lightweight 6061-T6 aluminum sheets can be used as transport buckets provided the construction includes the use of an aluminum honeycomb sandwiched between the 6061-T6 aluminum sheets. Although no propagations occurred when this configuration was tested at 3.6 meters, without a full series of confirmatory tests, a firm safe separation distance cannot be reported.

5. A safe separation predictive tool has been developed which allows gross estimates to be made within the limits delineated.

6. Analysis of the data on the effect of ramp covering material indicates that if a light material is selected, the safe separation distances established in open air can be used within the ramp.

7. The primary effect on reducing the pressure environment created by the donor is to increase the safe separation distance.

8. A second order effect is the area density of the ramp covering material.

9. There is no significant difference in safe separation distance from the use of Styrofoam, acoustic blanket, or corrugated fiberglass panels.

10. Material selection may be based on cost and utility considerations, as long as the area density is below 0.8 kg/m^2.

RECOMMENDATIONS

1. Consideration be given to the design of new conveyor systems to eliminate fragment hazards created by steel straps that circumvent conveyor buckets.
2. Thermoplastic buckets manufactured for use in-plant should be injection molded and have a wall thickness of not less than 6.4 mm.
3. The ramp covering may be selected on the basis of cost, maintenanance and life factors, as long as it has a low area density.
4. A safe separation predictive model should be expanded and developed to include additional materials and conditions.

REFERENCES

1. ARLCD-CR-8007, Slater, F. E., Bergmann, E. P., Rindner, R. M., Seals, W. O., "Development of Safe Separation Criteria for the Manufacture of BLU Bomblets," June 1980.

2. ARLCD-CR-78012, Wenzel, A. B., Rindner, R. M., "The Effects of Shielded Tote Bins on the Safe Separation of 168 Pounds of Composition A-7 Explosive," September 1977.

3. NWLR 1821, Johnson, C., Moseley, J. W., " Preliminary Warhead and Terminal Ballistic Handbook," March 1964.

4. ARLCD-CR-78021, Gehring, J. W., Rindner, R. M., Seals, W. O., "Safe Separation of Aluminum Tote Bins Containing Composition A-7," September 1978.

5. Interim Report, TM2189, Seals, W. O., Kukuyka, R. S., Rindner, R. M., Sarrett, H., "Safe Separation of Composition A-7 Explosive in 165 Pound Tote Bins," October 1975.

6. AMCP 706-180, "Engineering Design Handbook, Principles of Explosive Behavior," April 1972.

TABLE 1

PHYSICAL PROPERTIES

Material		Tensile Strength (TS) (psi)	Tensile Modulus (TM) (psi x 10^6)	Flexural Strength (FS) (psi)	Flexural Modulus (FM) (psi x 10^6)	IZOD Impact Strength Notches (ISN) (ft-lb/in.)	IZOD Impact Strength Unnotched (ISU) (ft-lb)
Polypropylene	RTP199X22898[1]	7,400	0.7	10,500	0.52	0.7	4.5
	RTP199X23835[1]	5,500	0.6	8,000	0.48	0.5	4.0
	RTP199X28016[1]	5,000	0.35	8,500	0.30	0.3	7.0
	RTP199X28017C[1]	4,000	0.7	7,000	0.55	0.5	3.5
ABS Type 752[2]		4,500 To 8,500	0.26 To 0.29	7,500 To 11,000	0.37 To 0.45	8.5	No Data
Lexan (Standard Grades)[3]		9,000	0.34	13,500	0.32	14.0	No Break
6061-T6 Aluminum[4]		45,000	10.0	45,000	10.0	No Data	No Data

1. Data from Fiberite Corporation, Winona, Minn.
2. Data from Monsanto Polymers & Petrochemicals, St. Louis, Mo.
3. Data from General Electric, Plastics Division, Pittsfield, Mass.
4. Data from <u>Machine Design</u>, Materials Reference Issue, 1978.

Table 2. Arena Tests of Potential Materials for Transport Buckets

TEST NO.	MATERIAL	NO. OF PENETRATIONS IN WITNESS PANEL	DEPTH OF PENETRATION INTO CELLOTEX	REMARKS
1	3.2 mm 6061-T6 Aluminum	15	114.3 mm	Witness panel received an additional 45 hits from fragments which did not penetrate.
2	1.6 mm 6061-T6 Aluminum	9	50.8 mm	Witness panel received an additional 13 hits from fragments which did not penetrate.
3	1.6 mm core Aluminum honeycomb between 1.6 mm 6061-T6 Aluminum plates	9	88.9 mm	The nine penetrations recorded were through the front panel only. One fragment did penetrate the rear panel of 1/16 in. aluminum.
4	3.2 mm core Aluminum honeycomb between 1.6 mm 6061-T6 Aluminum plates	10	25.4 mm	The aluminum honeycomb was flattened between the aluminum plates indicating considerable energy absorption. Of the 10 fragment penetrations, only the front 1/16 in. aluminum plate was pierced.
5	6.4 mm thick Acrylonitrile Butidienne Styrene (ABS)	0	25.4 mm	The witness panel received nine fragment hits but there were no penetrations.
6	Polycarbo- te 6.4 mm thick (Lexan)	0	50.8 mm	16 fragment hits were noted on the witness panel one of which almost achieved total penetration.
7	Polypropylene, 6.4 mm thick	0	25.4 mm	Witness panel fractured into several pieces either from impact or the blast wave. This phenomenon was determined to be unsatisfactory for transport buckets.
8	Polyphenylene Sulfide (Ryton), 6.4 mm thick	0	50.8 mm	27 fragment impacts were recorded with no penetrations. However some of these impacts caused the witness panel to shatter into six pieces. This material is too brittle for practical use.

Table 3. Bucket Fragment Data

BUCKET MATERIAL	AVERAGE FRAGMENT MASS	LARGEST FRAGMENT MASS	SMALLEST FRAGMEMT MASS	AVERAGE FRAGMENT LENGTH	AVERAGE FRAGMENT WIDTH	AVERAGE FRAGMENT THICKNESS	NO. OF FRAGMENTS IN	WALLBOARD PENETRATION
	GRAMS	GRAMS	GRAMS	MM	MM	MM	SAMPLE	MM
ABS	.136	.402	.065	9	7	5	11	25
LEXAN	.175	.480	.084	10	8	6	8	25
	.350	.628	.084	14	10	8	9	38
	.641	1.231	.045	14	10	9	2	51
RYTON	.045	.065	.006	5	4	3	8	25
	.104	.123	.091	7	5	4	3	38
	.071	.091	.045	6	4	4	3	51
POLY-PROPYLENE	.162	.434	.071	10	7	6	19	25
	.266	.369	.136	12	10	6	3	38
HONEYCOMB[1]	.071	.078	.065	6	6	2	2	89
HONEYCOMB[2]	.019	.032	.006	3	2	1	10	13
	.052	.065	.045	5	3	1	3	25
2 MM THICK ALUMINUM PANEL 6061-T6	.091	.136	.065	8	6	1	6	25
	.071	.084	.052	7	4	1	4	38
	.058	.110	.026	7	5	1	5	51
3 MM THICK ALUMINUM PANEL 6061-T6	.130	.466	.032	8	6	2	8	38
	.097	.162	.039	7	5	2	14	51
	.194	1.030	.032	8	6	3	17	63
	.162	.272	.084	8	6	3	11	76
	.356	.356	.356	15	9	3	1	89
	.363	.363	.363	14	8	5	1	102
	.071	.071	.071	7	5	3	1	114

1. 3 mm aluminum honeycomb, 13 mm thick, faced with 2 mm 6061-T6 aluminum sheets.
2. 10 mm aluminum honeycomb, 13 mm thick, faced with 2 mm 6061-T6 sheets.

Table 4. Estimated Impact Energy and Velocity

BUCKET MATERIAL	AVERAGE FRAGMENT MASS	CHARACTERISTIC FRAGMENT LENGTH ($\bar{L}$)	AVERAGE FRAGMENT DENSITY	ESTIMATED IMPACT VELOCITY	ESTIMATED IMPACT ENERGY	SCALED PENETRATION
	(GRAMS)	(MM)	(GMS/MM^3)	(M/S)	(GM-MM)	(P/$\bar{L}$)
ABS	.136	6	.000432	7	0.4	4
LEXAN	.175	6	.000364	6	0.3	4
	.350	9	.000312	5	0.5	4
	.641	9	.000509	16	8.5	6
RYTON	.045	3	.000750	36	2.9	8
	.104	4	.000743	40	8.4	9
	.071	4	.000739	49	8.8	13
POLY-PROPYLENE	.162	6	.000386	6	0.3	4
	.266	8	.000369	9	1.0	5
HONEYCOMB[1]	.071	4	.000986	94	31.8	22
HONEYCOMB[2]	.019	2	.003167	119	13.6	6
	.052	2	.003467	228	137.4	13
1/16 IN. ALUMINUM 6061-T6	.091	4	.001896	68	21.4	6
	.071	3	.002536	168	102.3	13
	.058	3	.001657	134	52.7	17
1/8 IN. ALUMINUM 6061-T6	.130	4	.001354	72	34.7	9
	.097	4	.001386	92	42.1	13
	.194	4	.001347	103	105.6	16
	.162	3	.001125	115	110.1	25
	.356	3	.000879	99	177.1	30
	.363	5	.000648	58	63.2	20
	.071	3	.000676	87	27.6	38

Table 5
Test Configuration: Safe Separation - Acrylonitrile Butadiene Styrene (ABS) Transport Buckets in Open-Air

SEPARATION DISTANCE	NUMBER OF TESTS	NUMBER OF DATA POINTS	NUMBER OF PENETRATIONS	NUMBER OF DETONATIONS	NUMBER OF BURNS	NUMBER OF NO PROPAGATIONS	PERCENT NO DETONATIONS	PERCENT NO BURNS	PERCENT NO PROPAGATIONS
2.4 m	1	1	---	1	0	0	0	0	0
3.6 m	9	9	0	0	0	0	100	100	100
4.9 m	1	1	0	0	0	0	100	100	100
6.1 m	1	1	0	0	0	0	100	100	100

Donor: 39.9 kg Composition B initiated at the bottom of the bucket utilizing a M-6 electric blasting cap in a 113 gram booster charge of Composition C-4.

Numerous fragment impacts were recorded on each acceptor at 3.6 m, 4.9 m and 6.1 m. One fragment penetrated into an acceptor bucket at 6.1 meters.

Table 6
Test Configuration: Safe Separation - Aluminum Transport Buckets with 9.5 mm Core of Aluminum Honeycomb, 12.7 mm Thick Sandwiched Between Plates of 1.6 mm Thick 6061-T6 Aluminum

SEPARATION DISTANCE (M)	NUMBER OF TESTS	NUMBER OF DATA POINTS	NUMBER OF PENETRATIONS		NUMBER OF DETONATIONS	NUMBER OF BURNS	NUMBER OF NO PROPAGATIONS	PERCENT NO DETONATIONS	PERCENT NO BURNS	PERCENT NO PROPAGATIONS
			FRONT PANEL	REAR PANEL						
3.6	2	2	34	2	0	0	2	100	100	100
4.9	2	2	29	0	0	0	2	100	100	100

Donor: 39.4 kg Composition B initiated at the bottom of the bucket utilizing a M-6 electric blasting cap in a booster charge of 113 grams, Composition C-4.

Table 7. Biomation Settings

CHANNEL NO.	TRANSDUCERS TYPE	LOCATION	SERIAL NO.	IN-LINE CONDITIONER SERIAL NO.	VOLTS f/s	VOLTS c/m	GAIN
1	LC-33	4.6 M	738	2595	0.5	0.25	1
2	LC-33	7.6 M	946	2599	2.0	1.0	1
3	LC-33	10.7 M	697	2598	0.5	0.25	1
4	---	---	---	---	---	---	---
4	1 kHz time signal						

Sweep Rate: Two MSEC/CM

Sample Interval 20MSEC

TABLE 8

RAMP PRESSURE - STANDOFF - MATERIAL DATA

Ramp Cover Material	Mat'l Area Density (ρ'_m) kg/m^2	Peak Side-On Pressure At Standoff (R) 4.6m	7.6m	(P_{so}), kPa 10.7m	ρ'_m/ρ_o
Open Air	0.122*	572	469	186	1.00
Styrofoam	0.312	N.D.**	441	N.D.	2.56
Corrugated Fiberglass	0.703	1234	469	172	5.76
"Rigid Board"	1.767	813	414	186	14.48

*kg/m^3 x .1M (Arbitrary)

**N.D. = No Data (Gauge Destroyed)

Table 9
Test Configuration: Safe Separation - Acrylonitrile Butadiene Styrene (ABS) Transport Buckets in Ramps

RAMP MATERIAL	NUMBER OF TESTS	NUMBER OF DATA POINTS	NUMBER OF PENETRATIONS	NUMBER OF DETONATIONS	NUMBER OF BURNS	NUMBER OF NO PROPAGATIONS	PERCENT NO DETONATIONS	PERCENT NO BURNS	PERCENT NO PROPAGATIONS	SEPARATION DISTANCE
Styrofoam (1)	9	17	2	0	0	17	100	100	100	3.66 meters
Styrofoam	1	1	0	1	0	0	0	0	0	3.0 meters
Acoustic Blanket (2)	2	4	2	0	0	4	100	100	100	3.66 meters
Corrugated Fiberglass (3)	2	4	0	0	0	4	100	100	100	3.66 meters

(1) Styrofoam - 1.2 meters x 2.4 meters x 25.4 mm (Size per sheet).

(2) Acoustic Blanket - 1.2 meters x 2.4 meters x 25.4 mm (spun fiberglass - size per sheet).

(3) Corrugated Fiberglass - 0.66 meter x 2.4 meters x 1.6 mm (size per sheet).

Hits on the acceptor buckets from fragments generated by the donor charge ranged from none to 22 with four penetrations noted.

TABLE 10

SAFE SEPARATION MODEL DATA BASE

Source Reference	Explosive	Bucket Material	Explosive Weight (c)** kg	Bucket Weight (m)kg	c/m	Bucket Mat'l Density (ρ_f) (lb/in.)	Bucket Thickness (t) (in.)	Bucket Flexural Modulus (E_F) (lb/in.^{2}x10^{-6})	Bucket Flexural Strength (σ_{uf}) (lb/in.^{2}x10^{-3})	X_{100} Experimental (m/kg$^{1/3}$)
1	Comp B	Steel	.031	.118	.26	.283	~.125	30	80	.03
1	A-7	304SS	79.4	18.5	4.3	.286	.083	29	75	9.40
1	Cyclotol	6061-T6 Al	29.5	4.3	6.9	.098	.118	10	45	3.02
*	Comp B	6061-T6 Al + Honeycomb	34.0	4.6	7.4	.010	.625	10	45	1.15
*	Comp B	ABS	34.0	3.5	9.7	.036	.250	.37	11	1.15
1	Cyclotol	Cardboard	29.5	1.8	16.5	.038	.125	Unknown	Unknown	2.18
1	Cyclotol	6061-T6 Al	29.5	1.4	21.2	.098	.039	10	45	2.42

*This Program

**TNT Equiv. (Ref. 6)

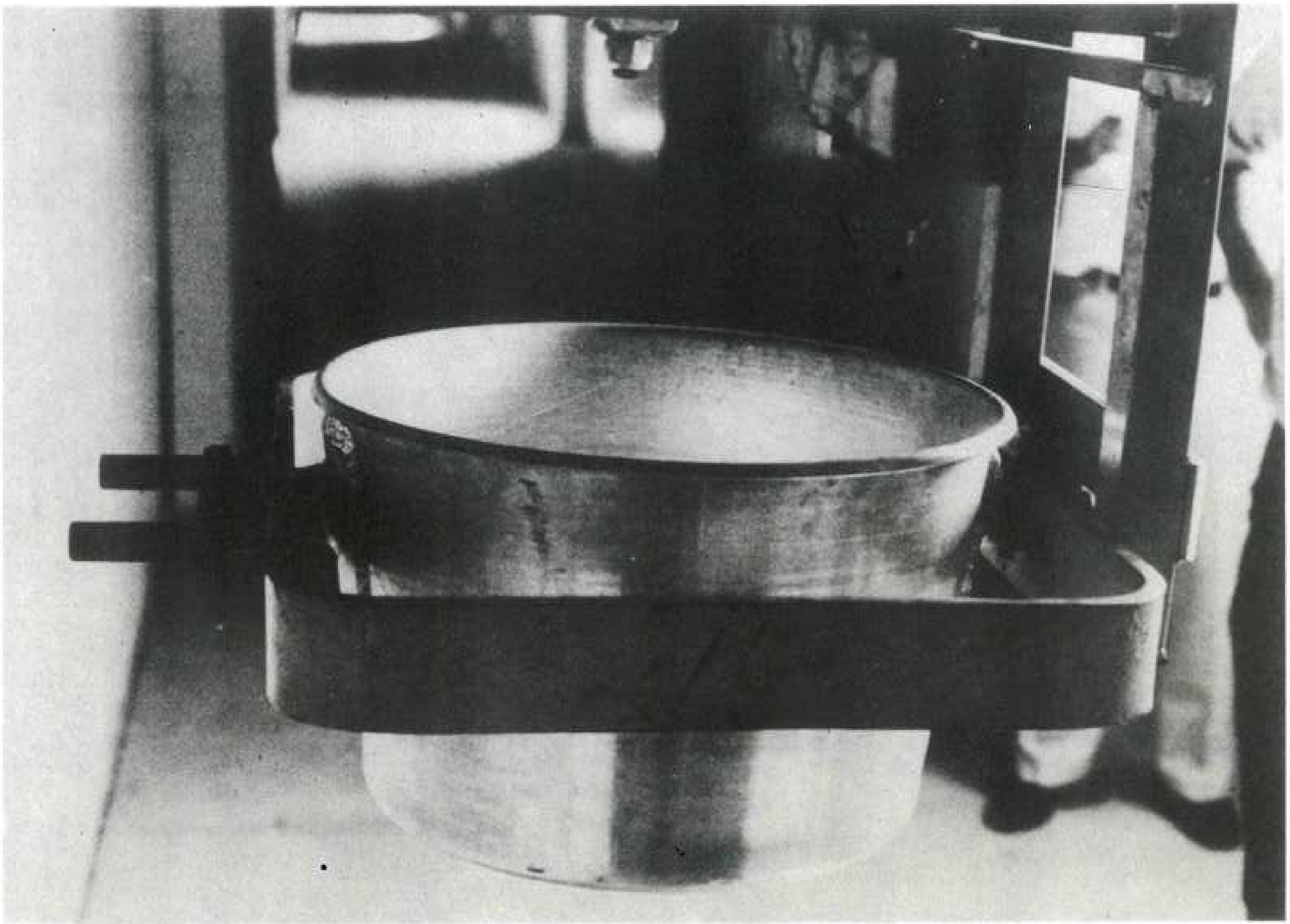

Figure 1. Typical Cylindrical Transport Bucket Currently in Use In-Plant

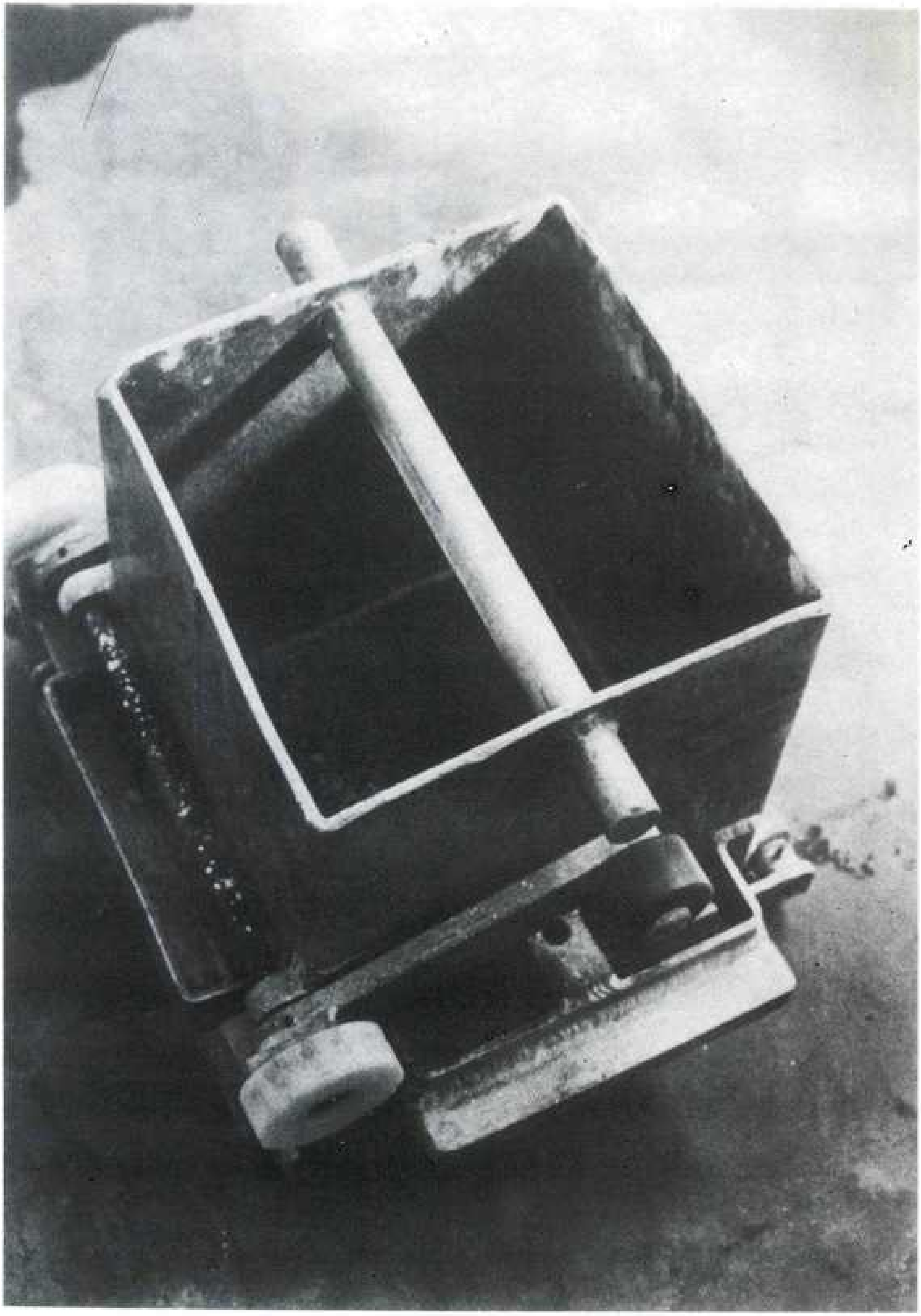

Figure 2. Typical Square Aluminum Transport Bucket Currently in Use In-Plant

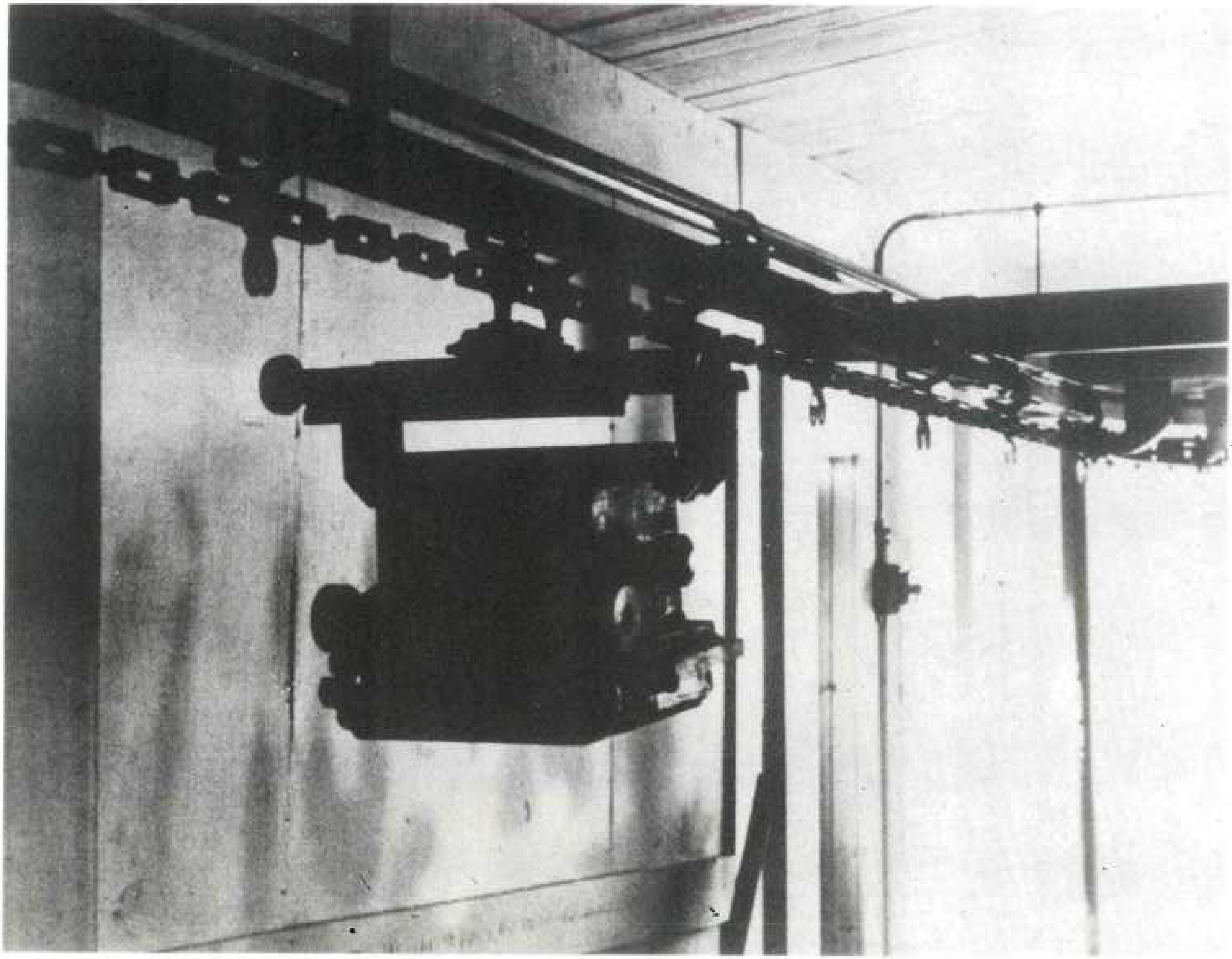

Figure 3. Typical Overhead Conveyance System

Figure 4. A Type of Ramp Construction with Overhead Conveyor System

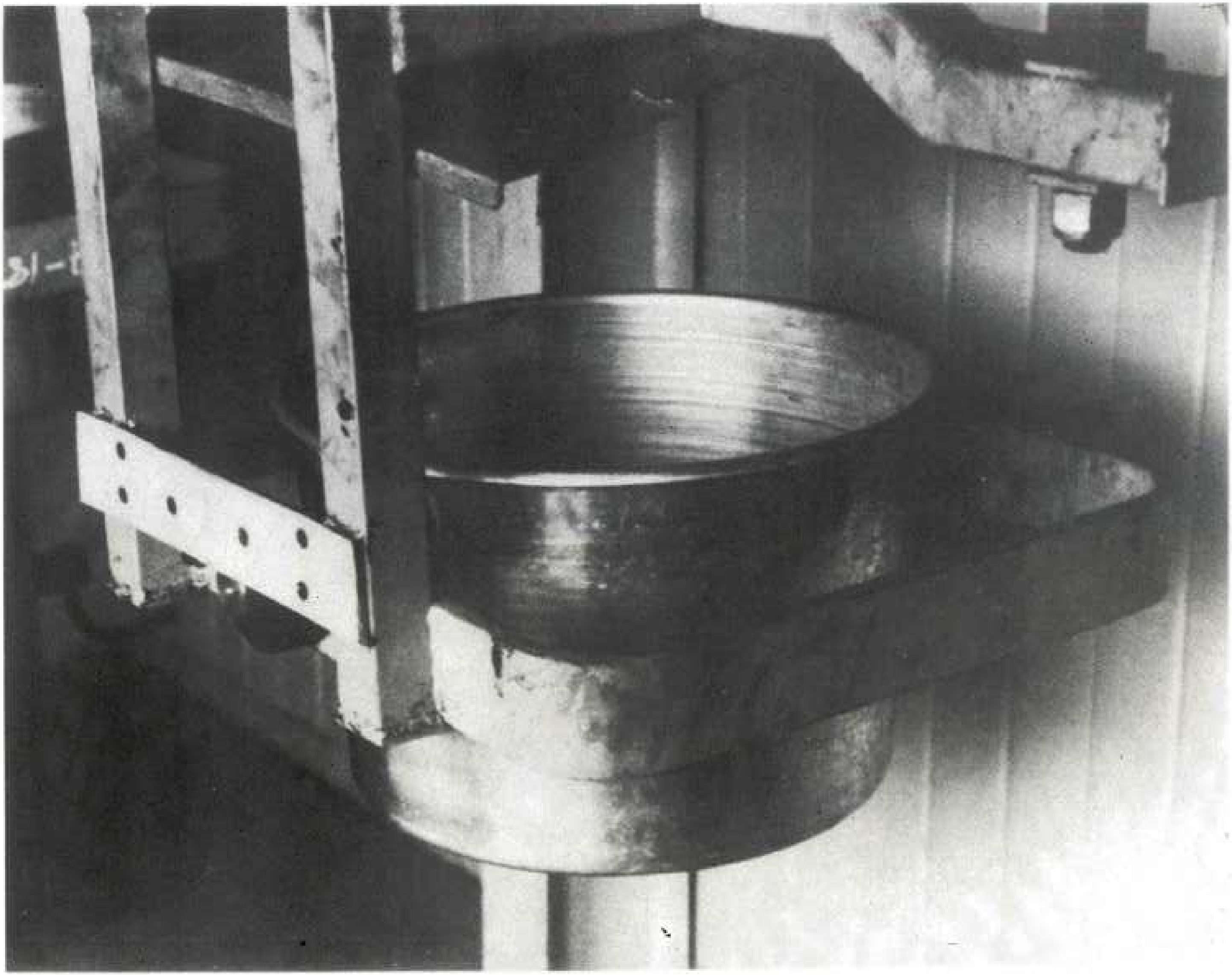

Figure 5. Example of Steel Strapping Circumventing Aluminum Transport Bucket

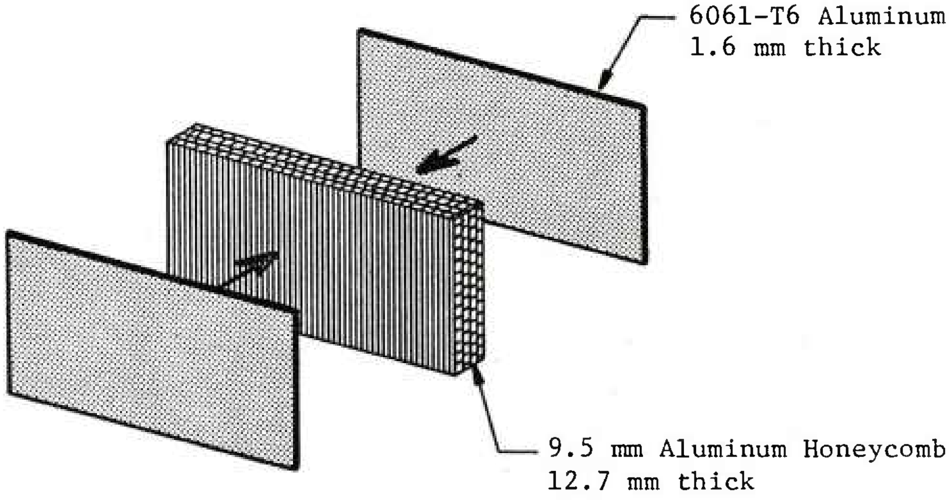

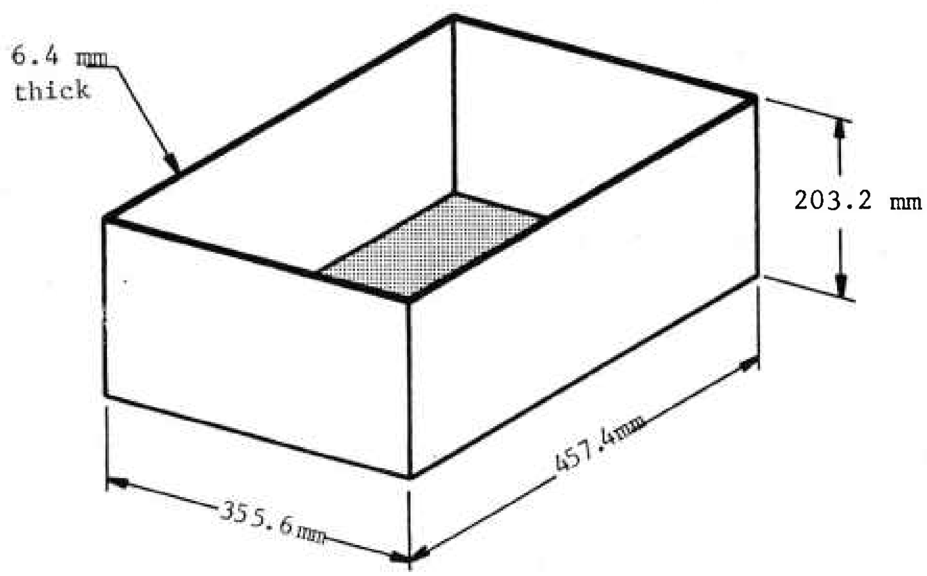

Figure 6. Bucket Configurations

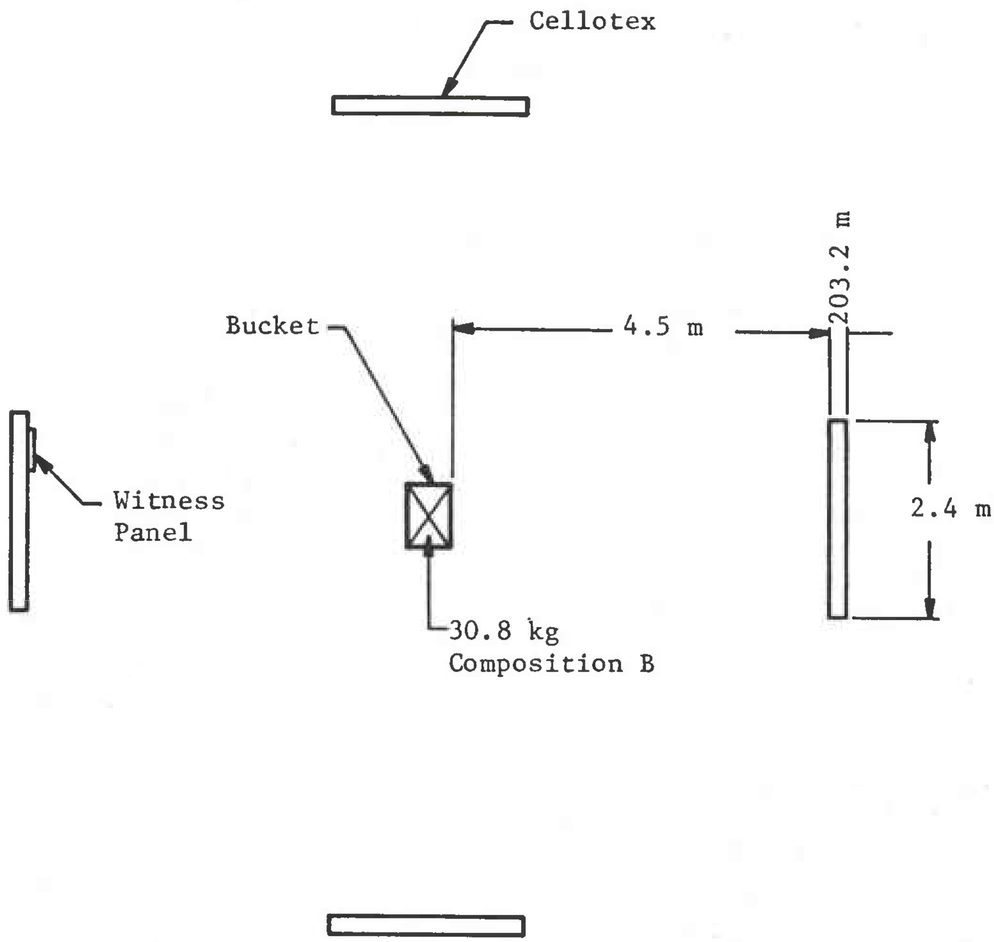

Figure 7. Test Set-Up (Arena)

Figure 8. Witness Panel

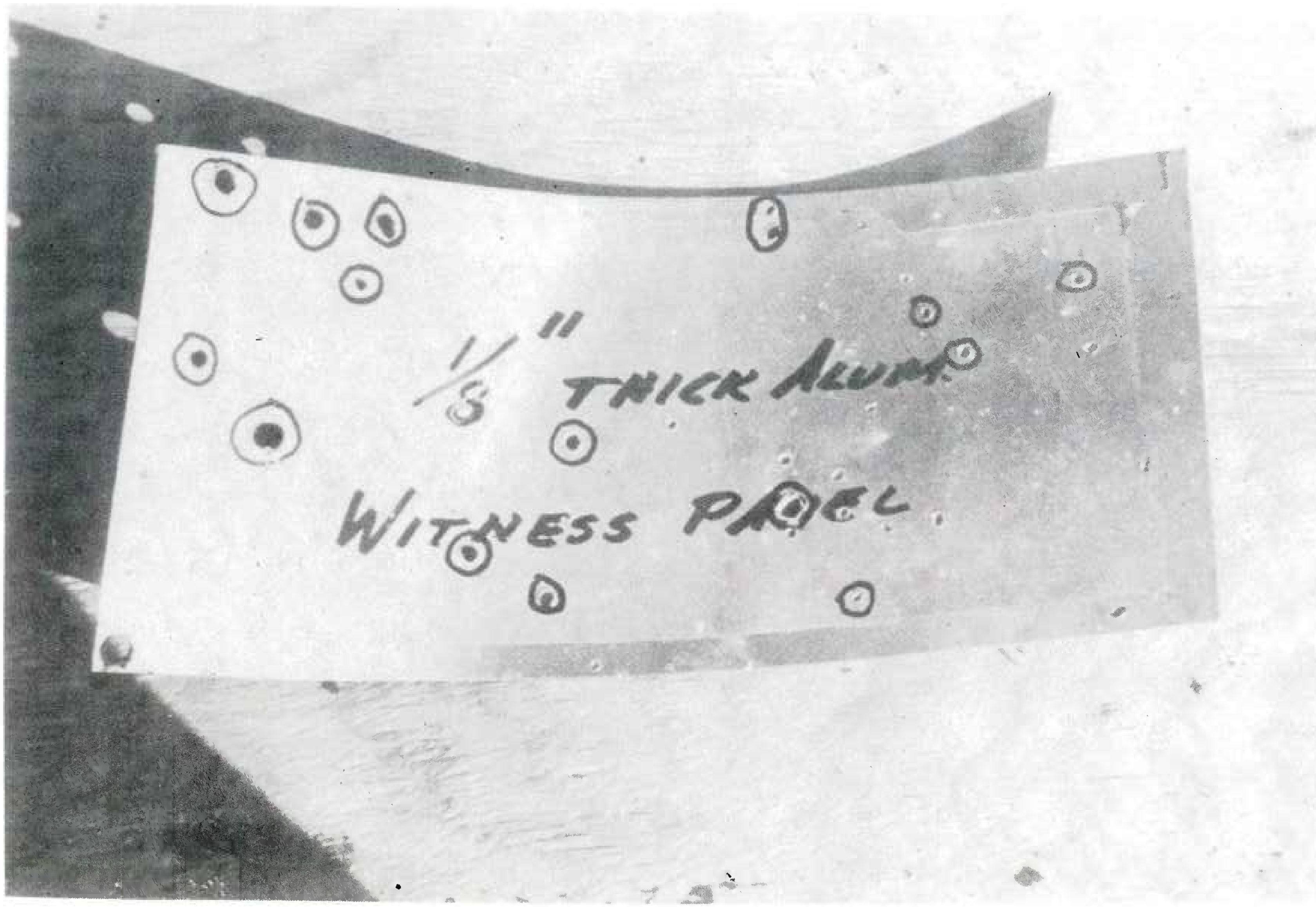

Figure 9. Severity of Fragment Impact on 3.2 mm Aluminum Witness Panel at 4.6 Meters

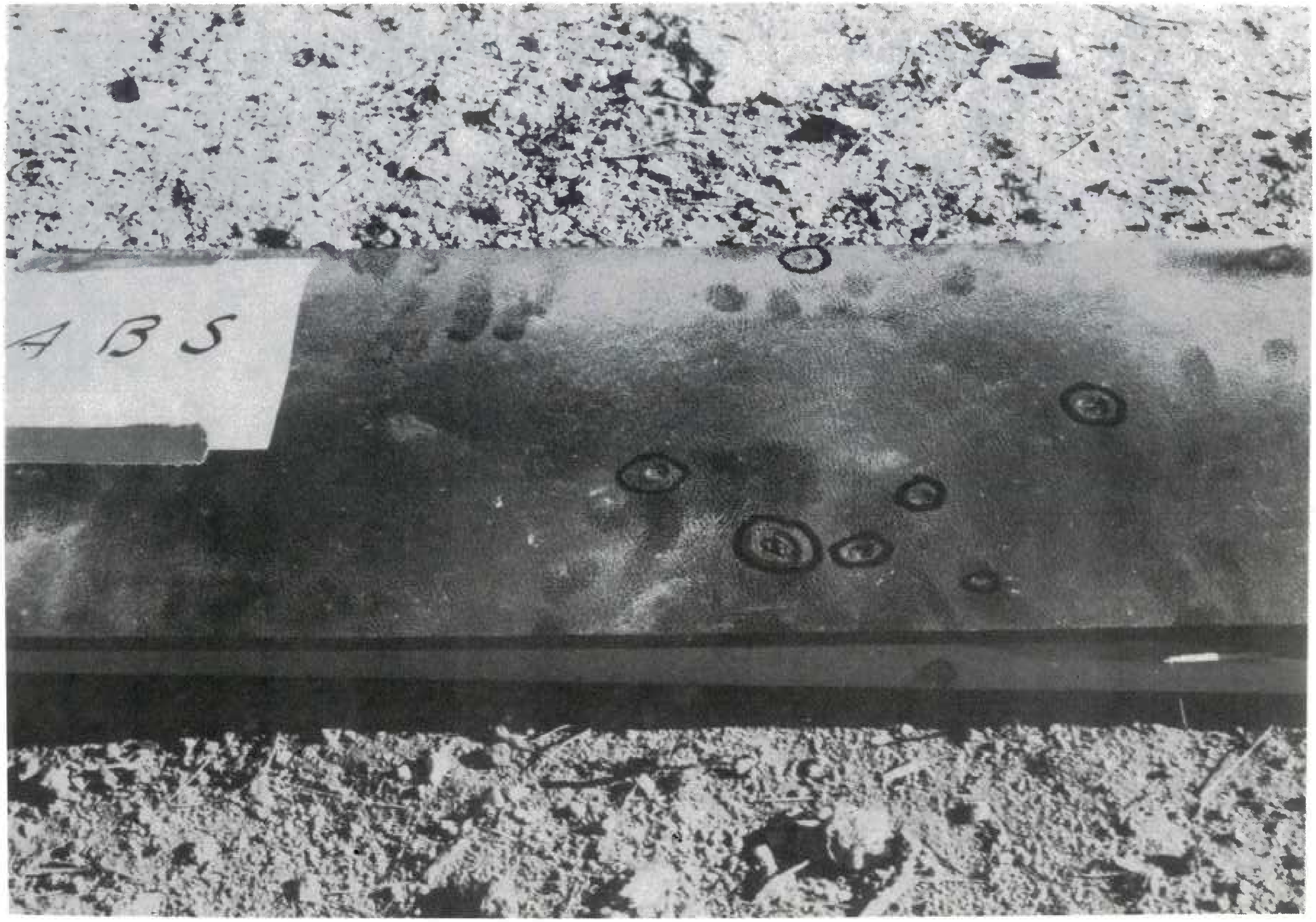

Figure 10. Typical Results Attained Using Acrylonitrile Butadiene Styrene Witness Panel. No Penetrations.

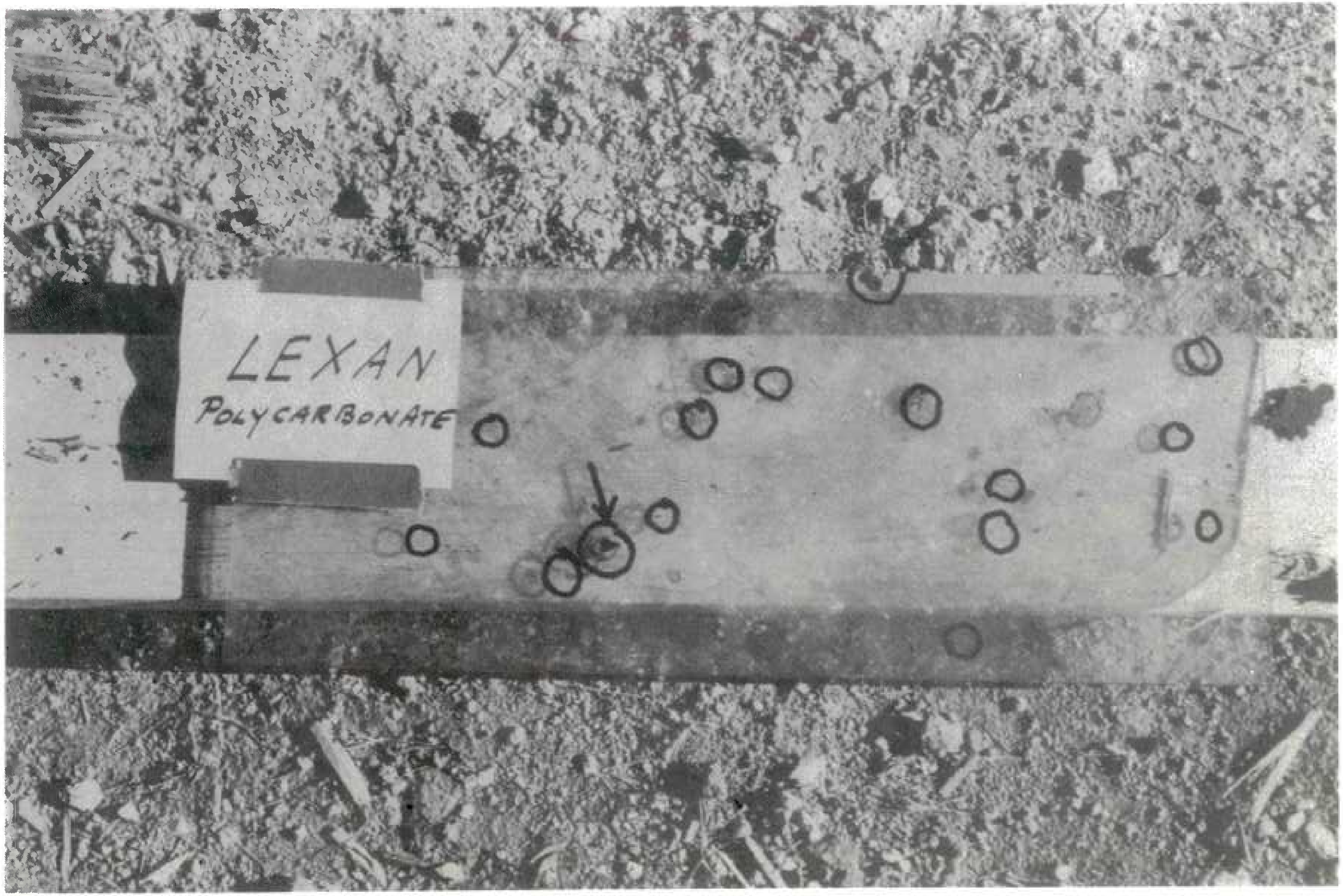

Figure 11. Typical Fragment Impacts on Polycarbonate (Lexan) Witness Panel. Note one Near Penetration.

Figure 12. Typical Results with The Polypropylene Witness Panel. Panel Shattered into Numerous Pieces from the Blast Pressures.

Figure 13. Fragment Impacts on Polyphenylene Sulfide. No Penetrations but Witness Panel Shattered from Blast Pressures.

Figure 14. Fragment Penetrations of the Front and Back Panel of the 1.6 mm Aluminum with 3.2 mm Aluminum Honeycomb

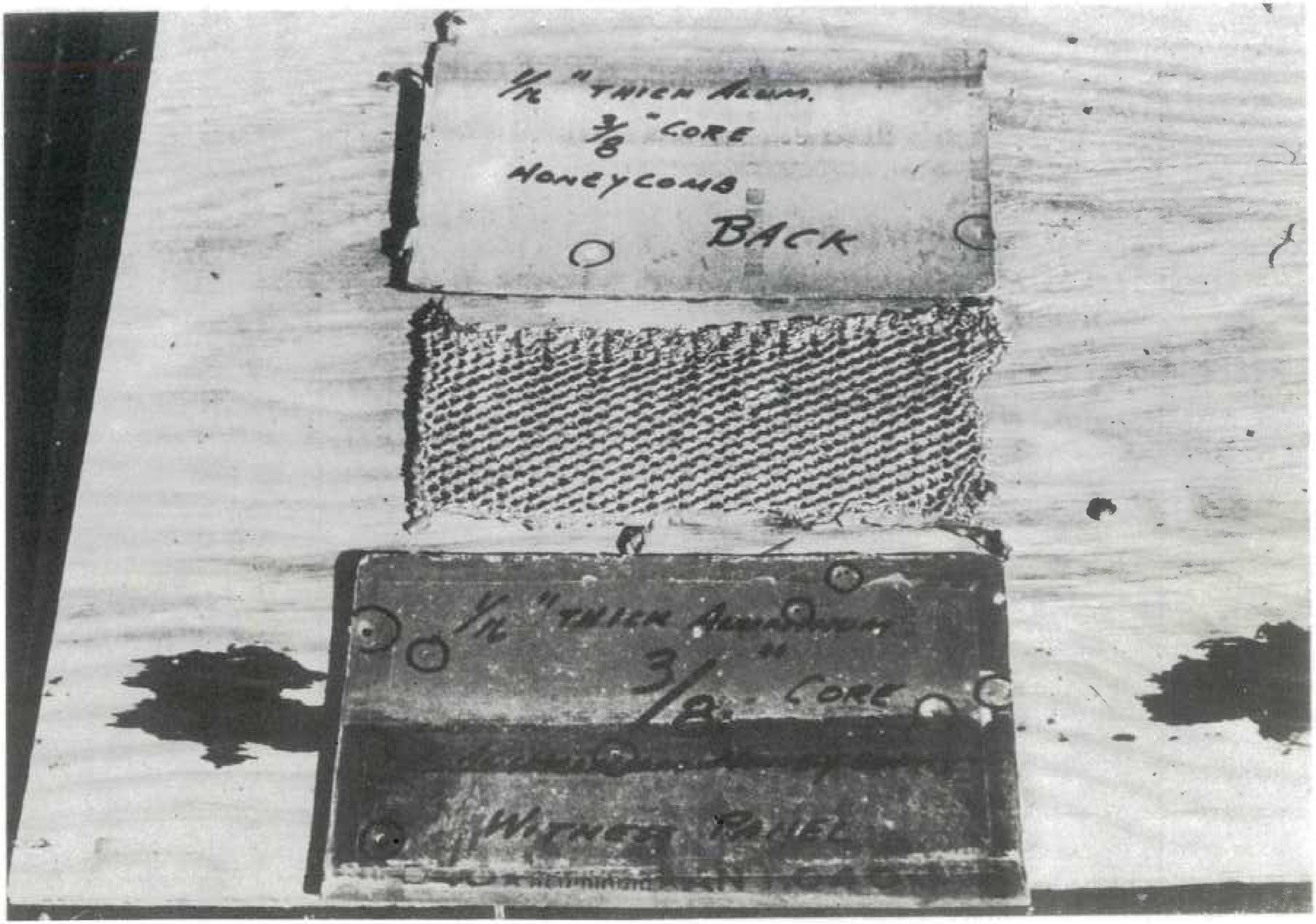

Figure 15. Fragment Penetrations of the Front Panel of 1.6 mm Aluminum with 9.5 mm Aluminum Honeycomb. No Penetration of Rear Panel.

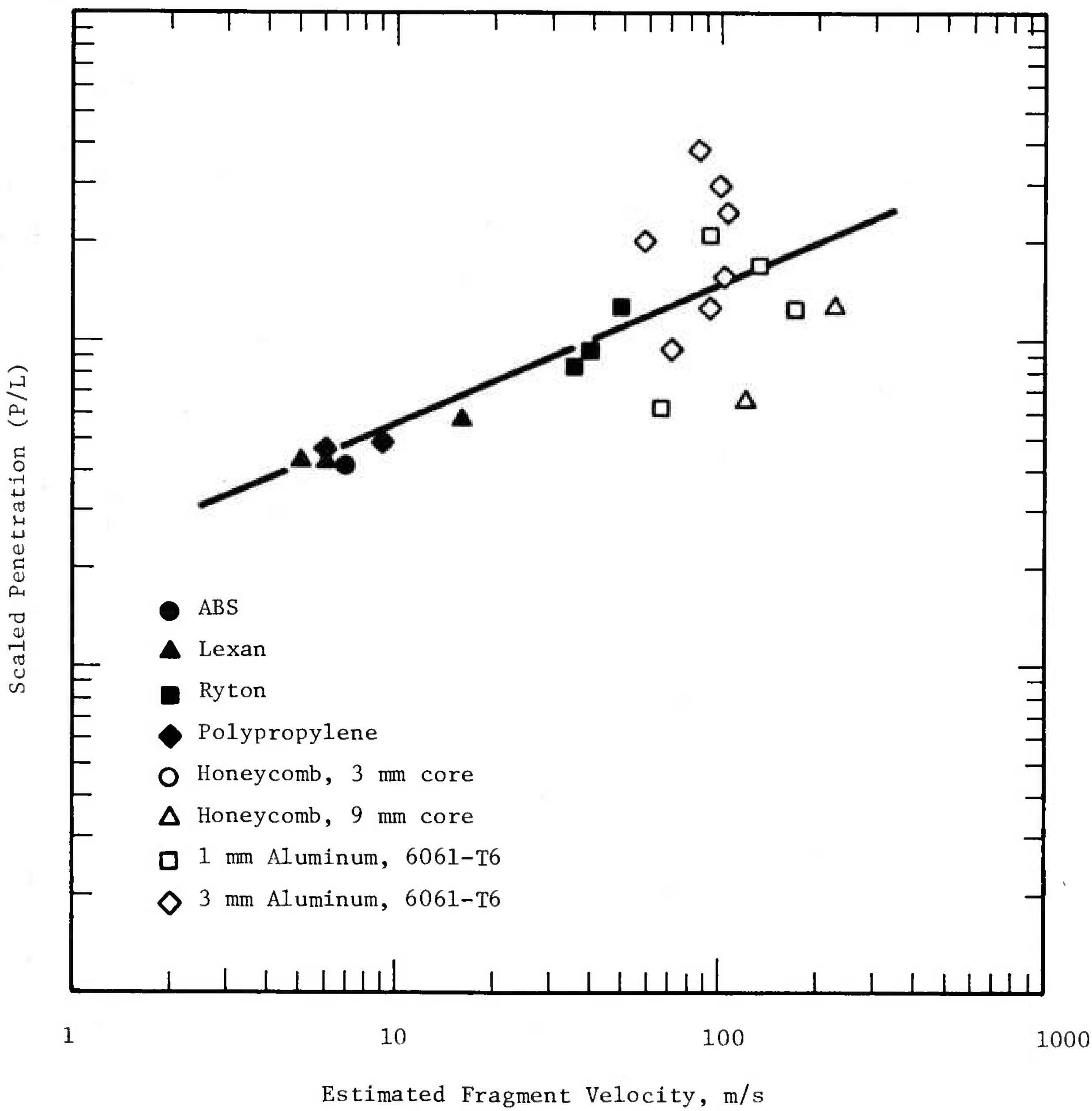

Figure 16. Scaled Penetration versus Estimated Fragment Velocity

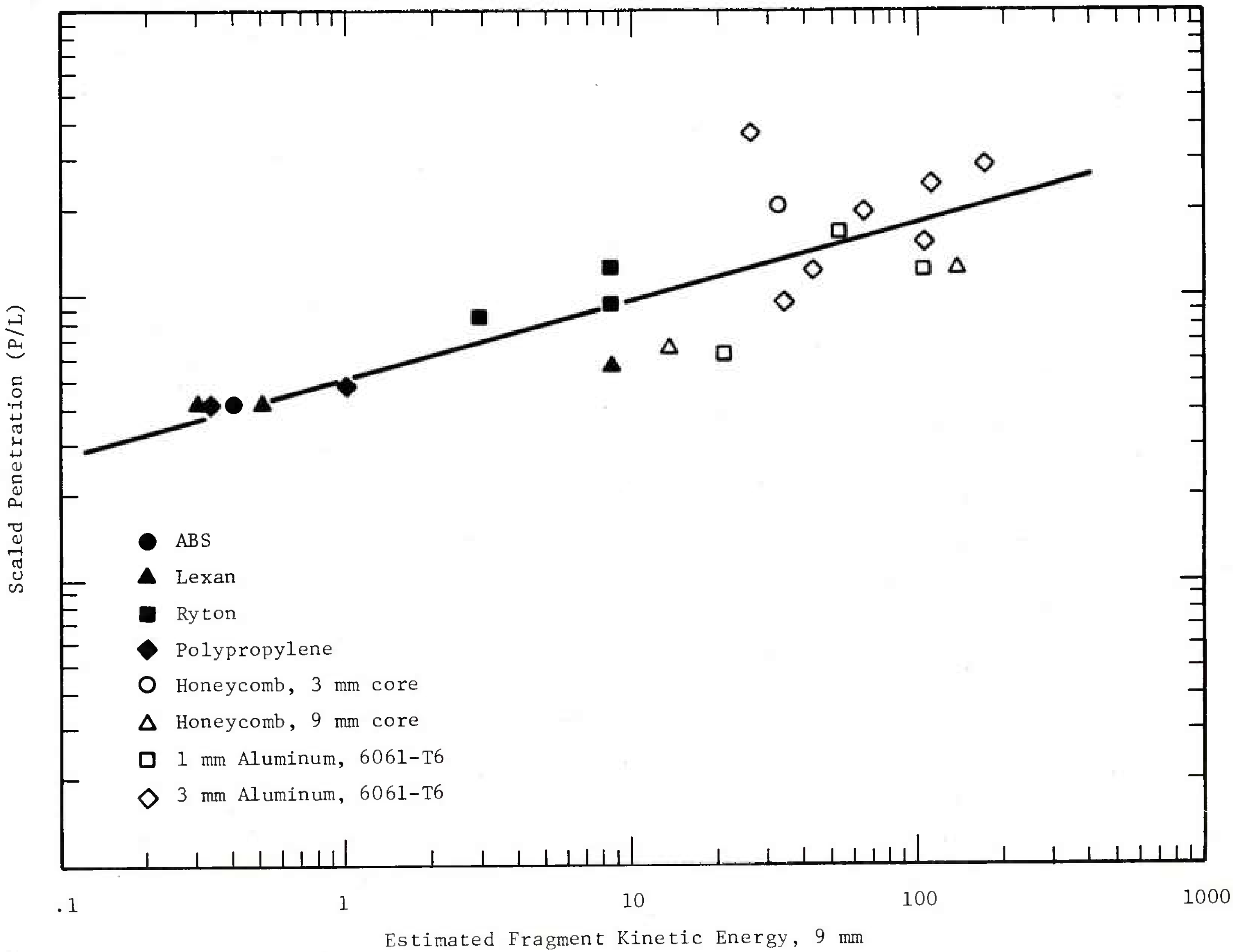

Figure 17. Scaled Penetration versus Estimated Kinetic Energy

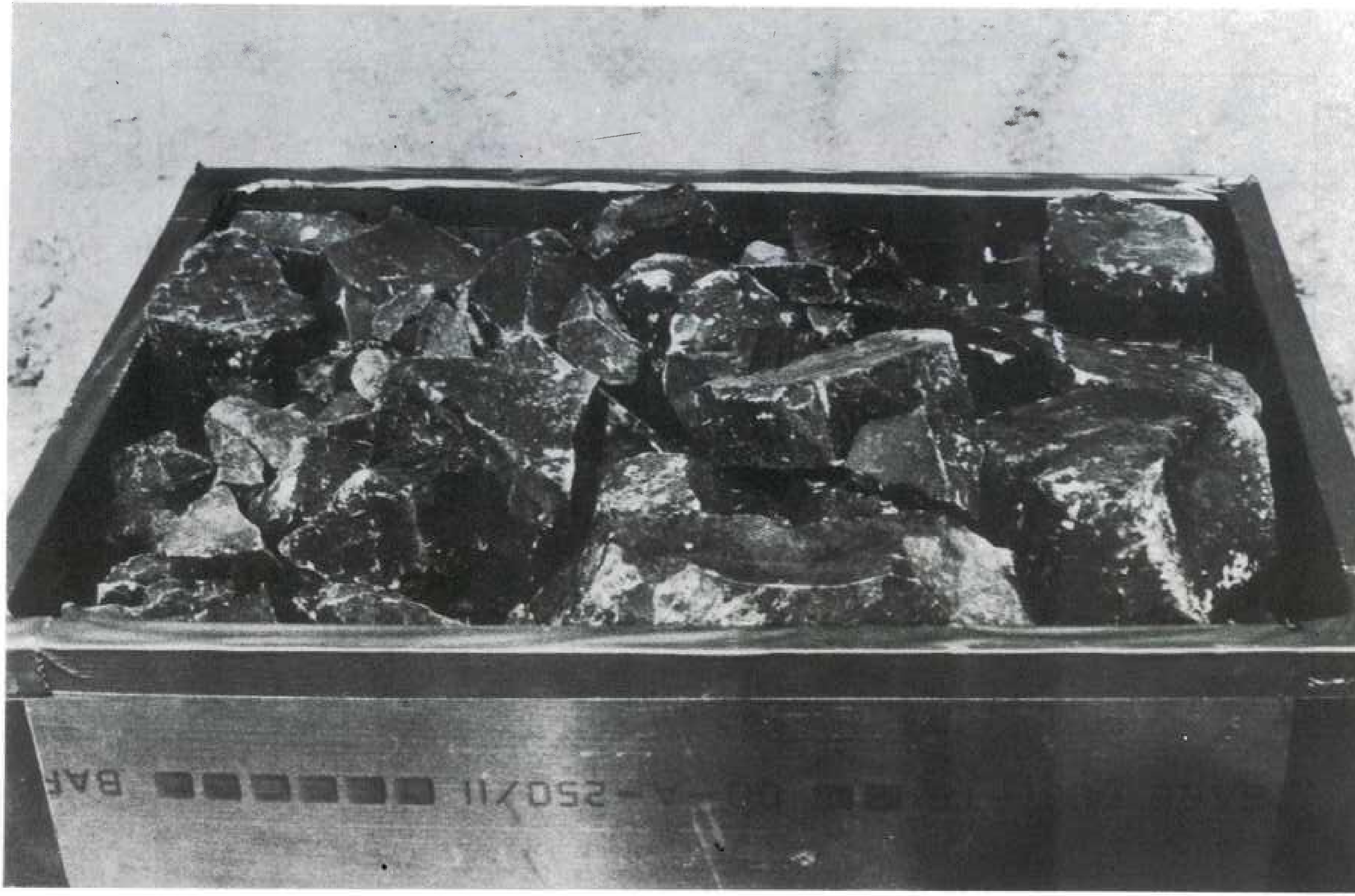

Figure 18. Aluminum Transport Bucket Filled with Comp B Explosive Utilizing 9.5 mm Aluminum Honeycomb Between 1.6 mm Aluminum Panels

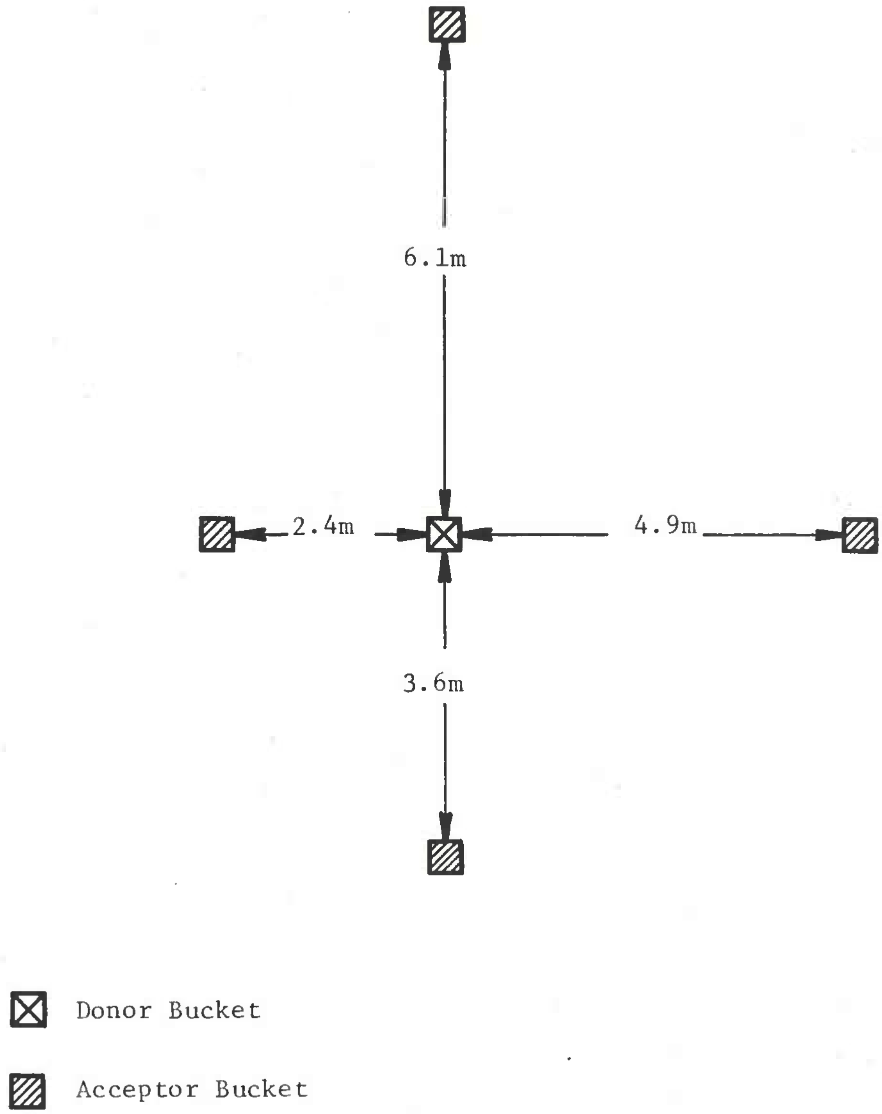

Figure 19. Test Set-Up to Establish Safe Separation Distances

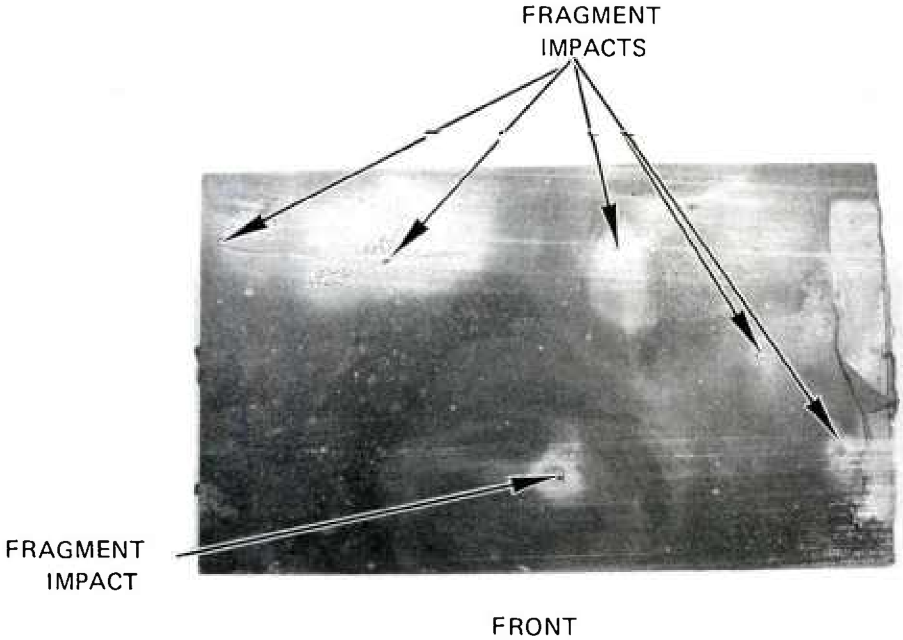

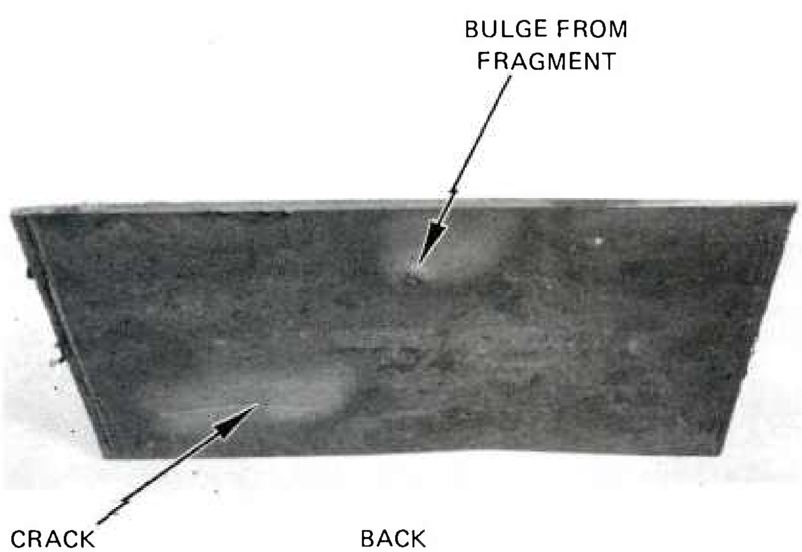

Figure 20. Typical Damage Sustained on Acceptor Bucket of ABS

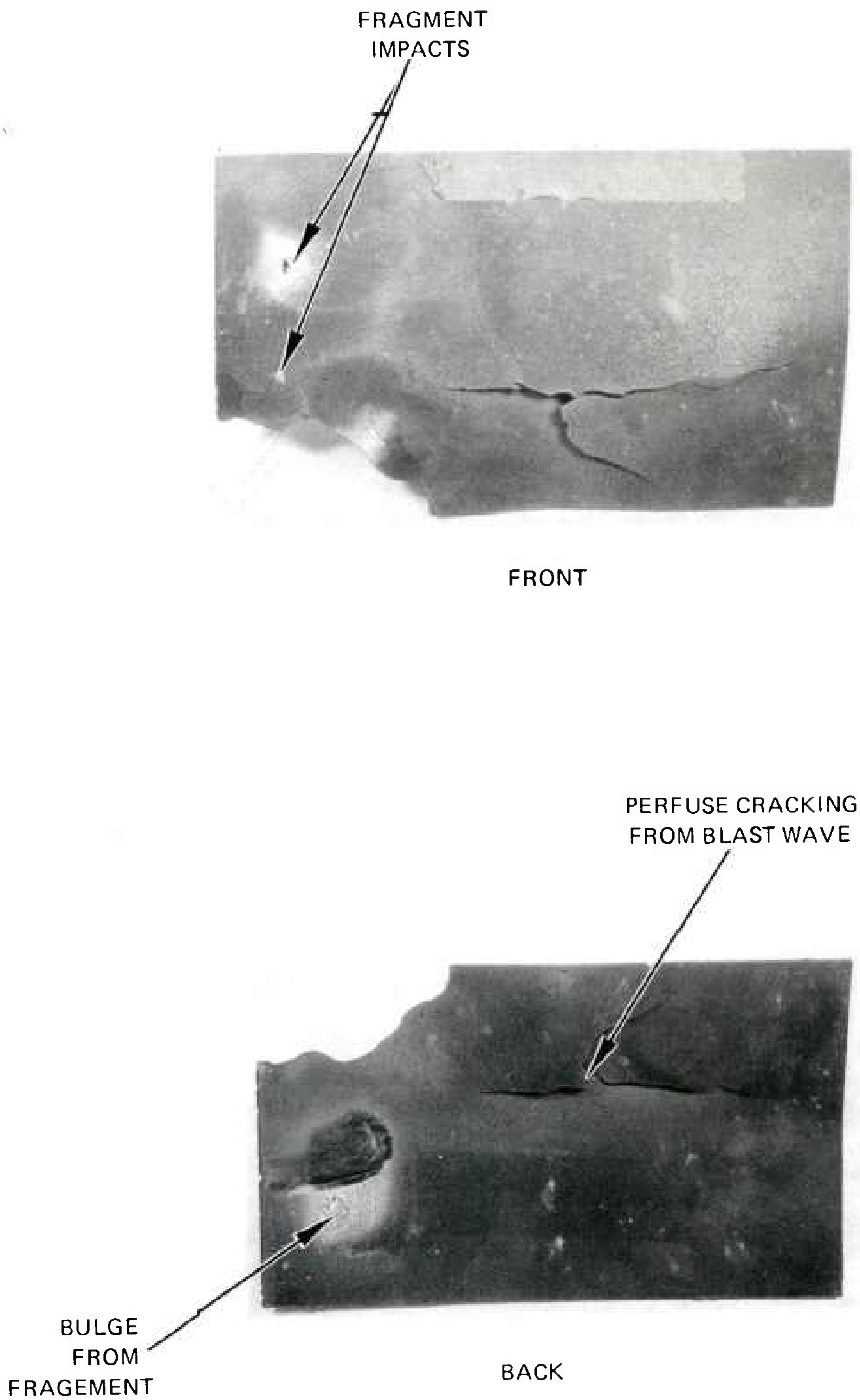

Figure 21. Severity of Damage Inflicted to Acceptor Bucket (ABS) at 3.6 Meters

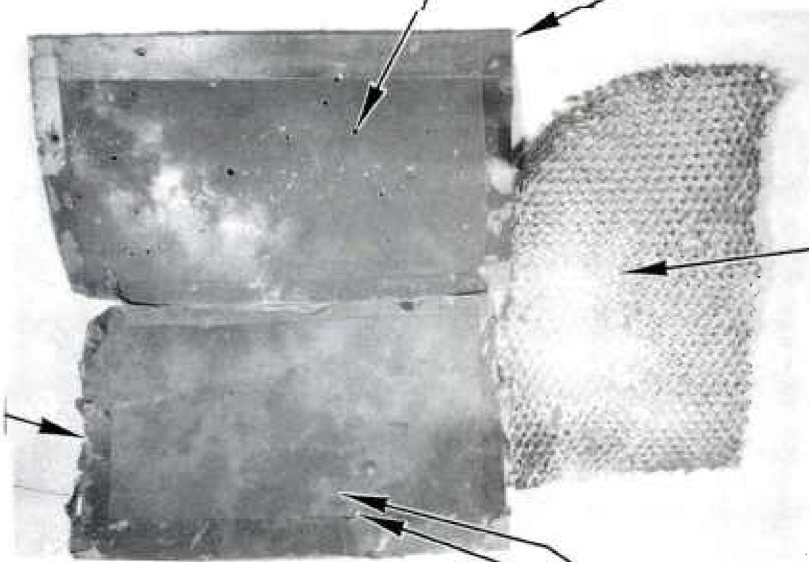

Figure 22. Fragment Penetrations of Aluminum Buckets with Honeycomb at 3.6 Meters

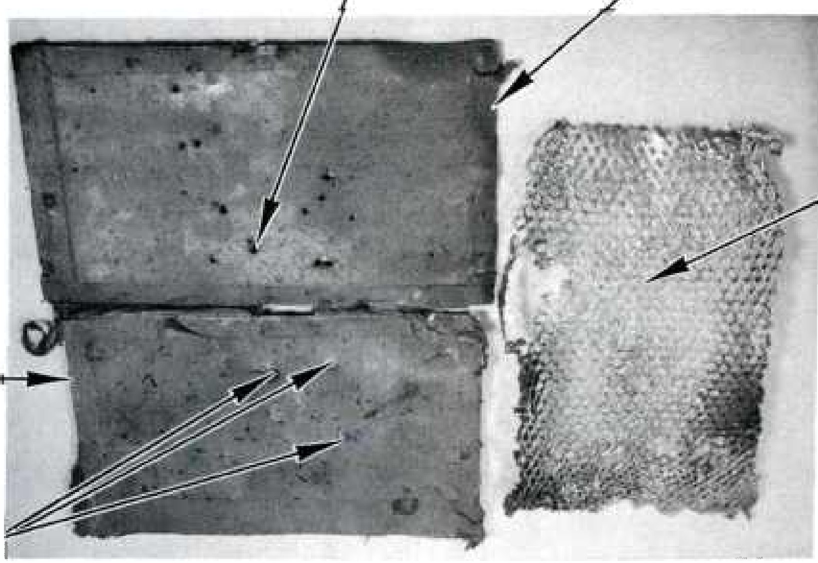

Figure 23. Fragment Penetrations of Aluminum Buckets with Honeycomb at 4.9 Meters

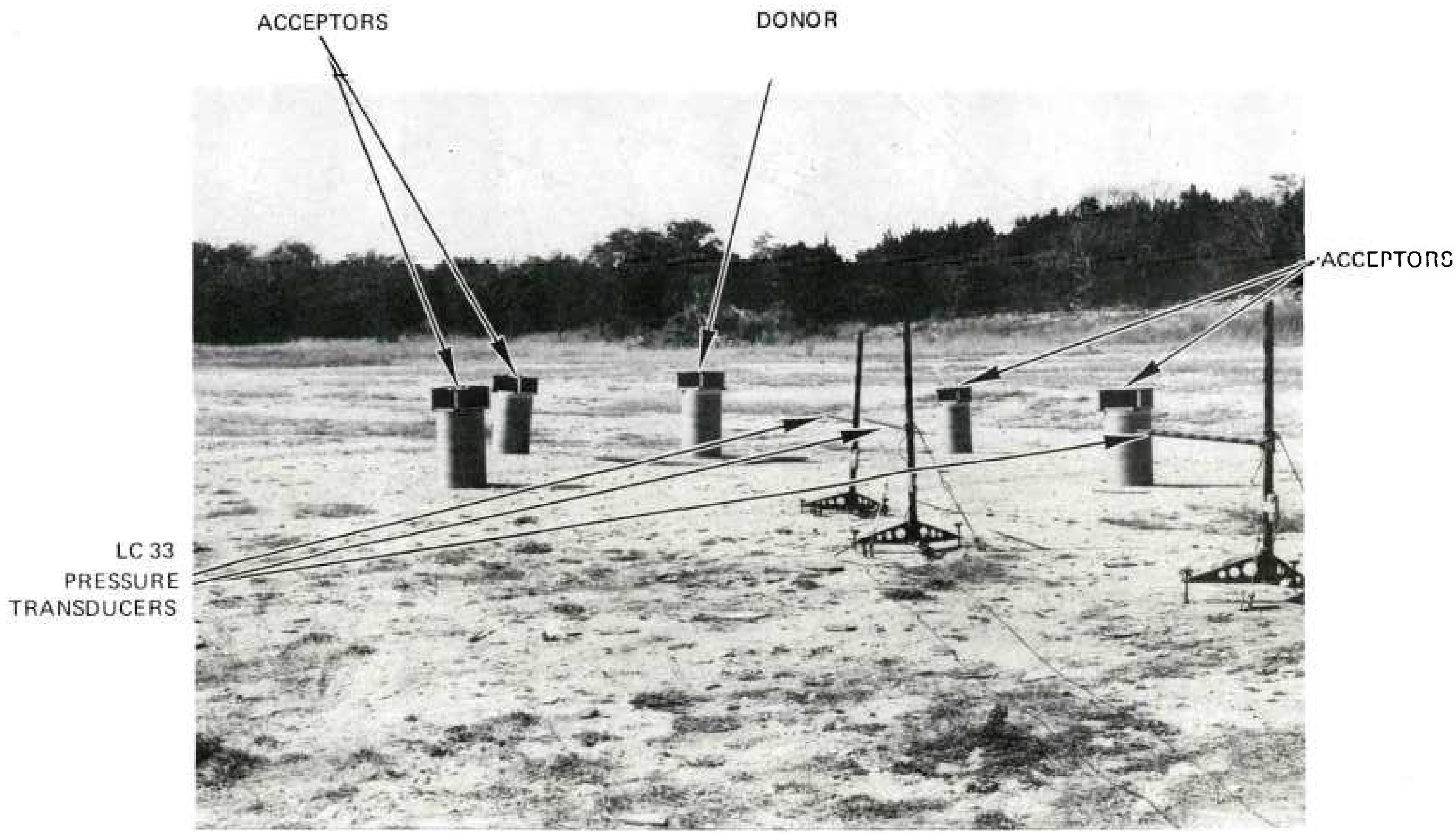

Figure 24. Typical Test Set-Up (Open-Air)

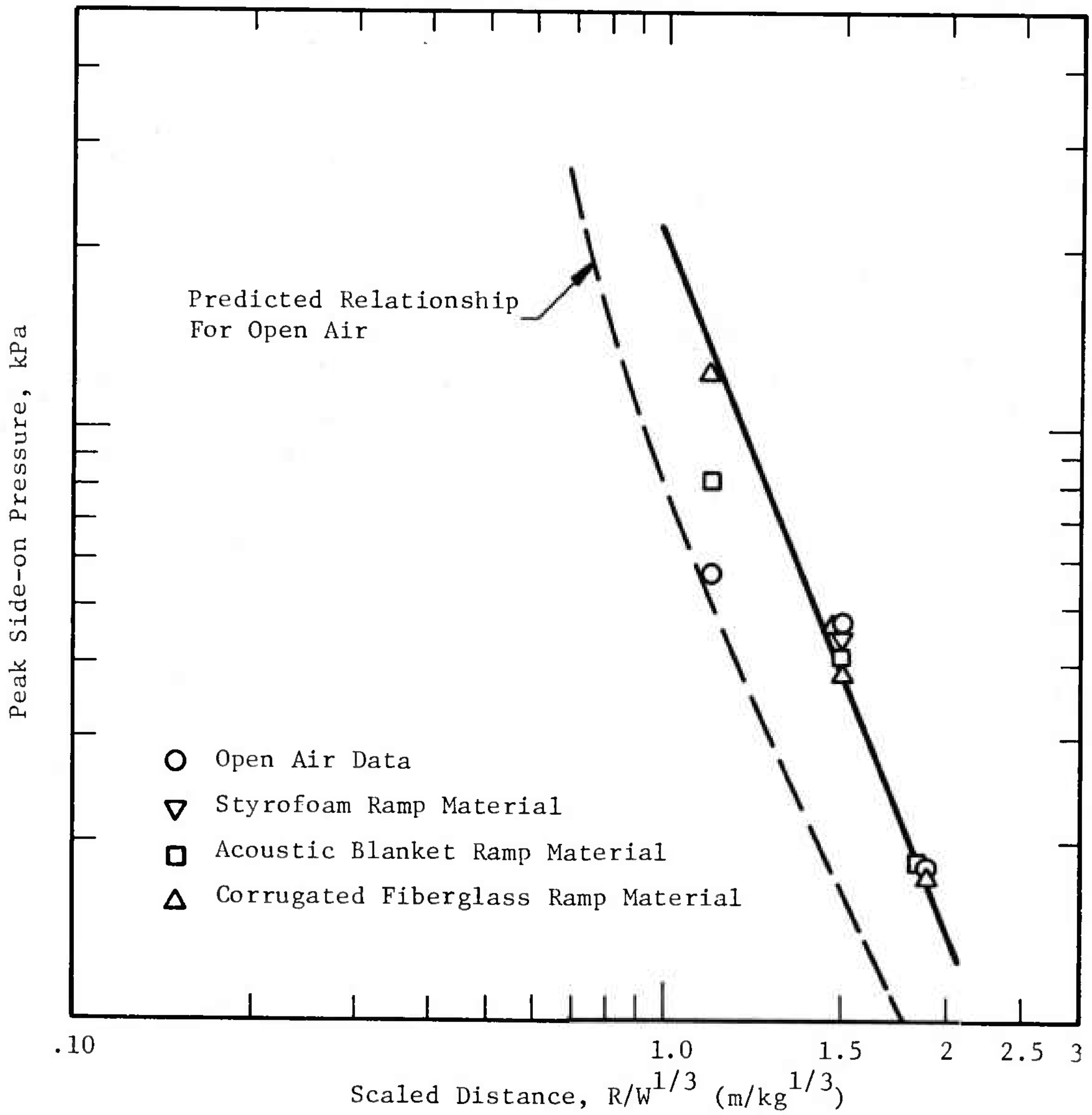

Figure 25. Peak Side-on Pressure Recorded

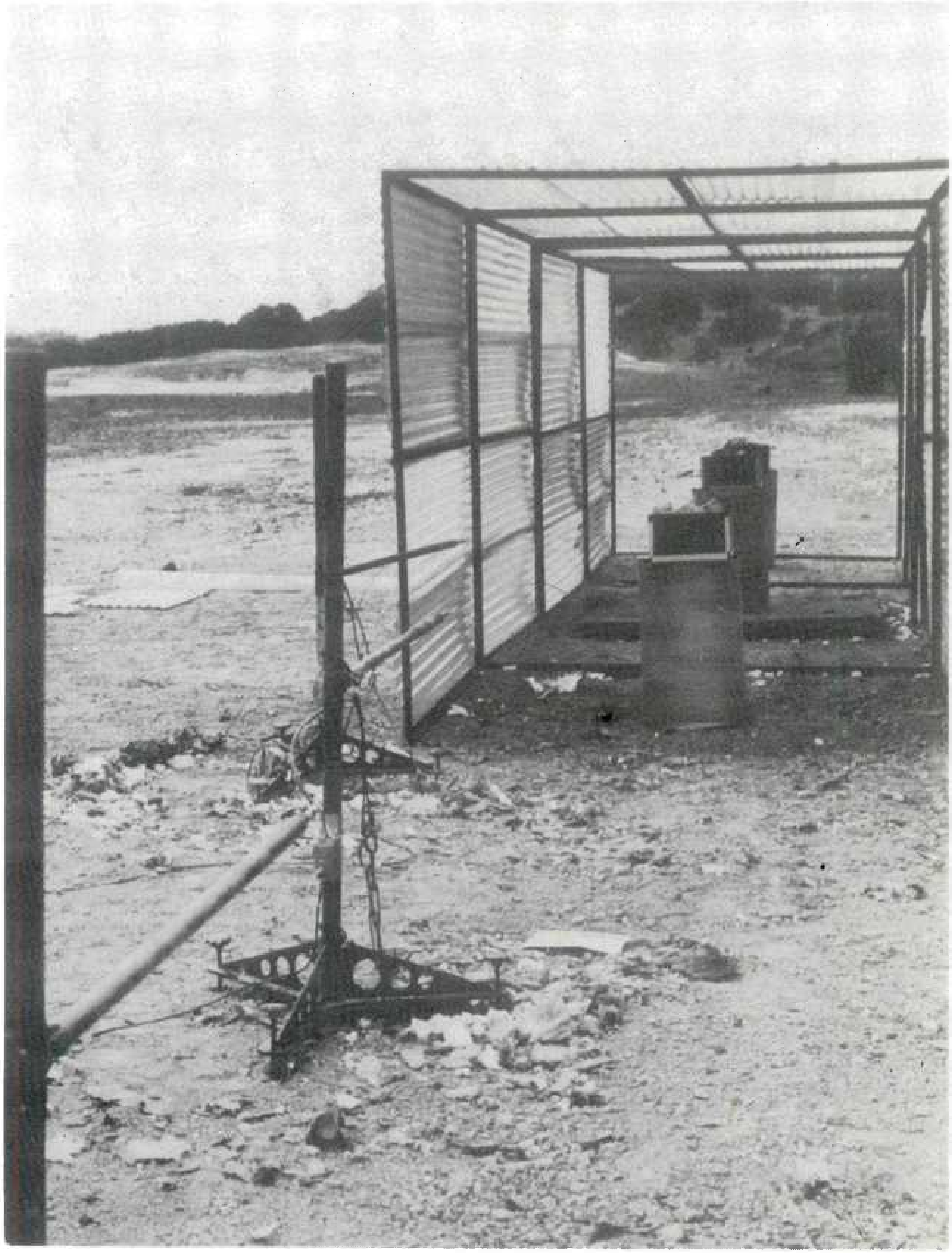

Figure 26. Typical Test Configuration for Ramp Tests

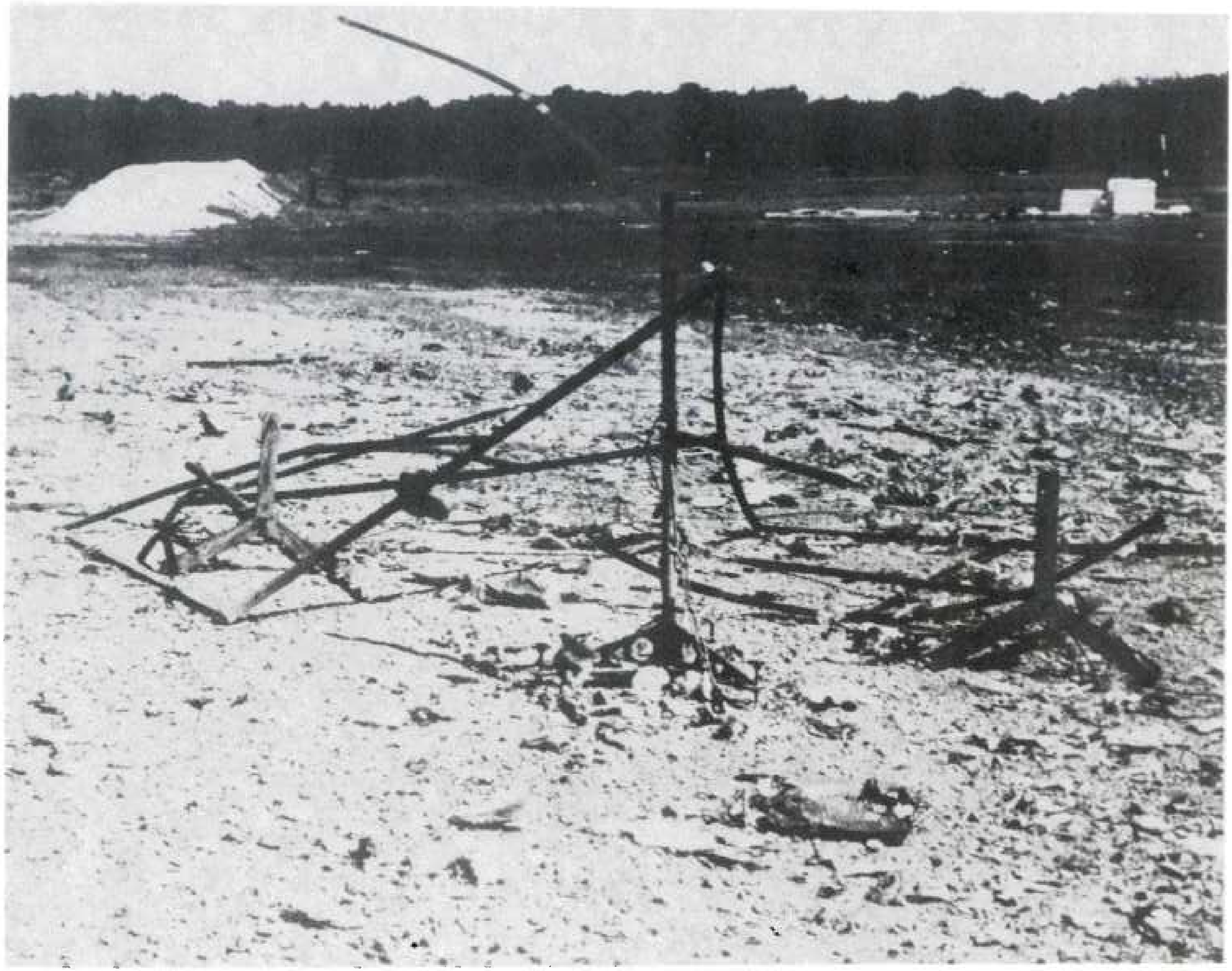

Figure 27. Depicts Total Destruction of the Ramp

Figure 28. Composition B Residue from Acceptor Bucket

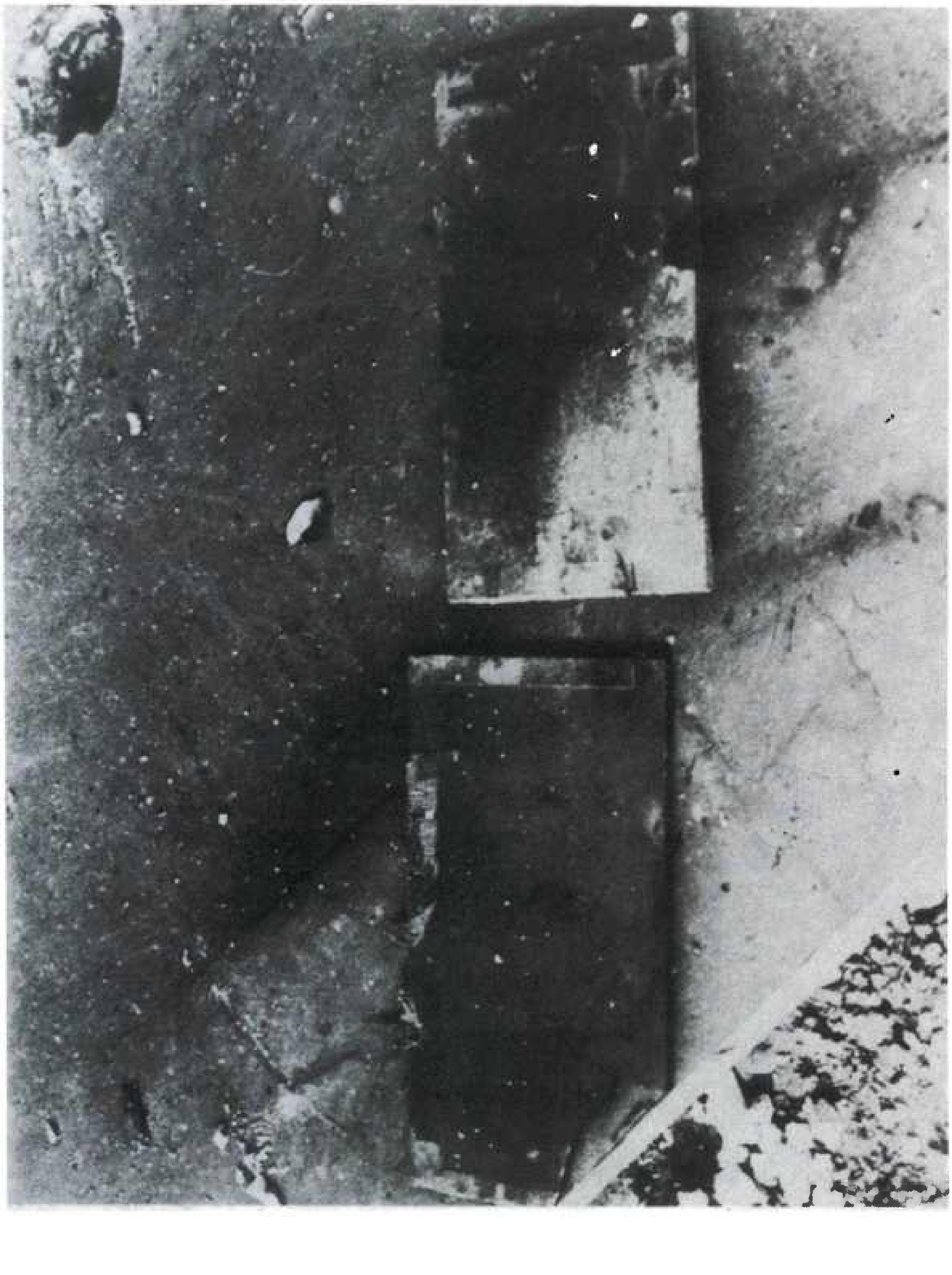

Figure 29. Typical Results Noted as a Result of Fragment Impacts

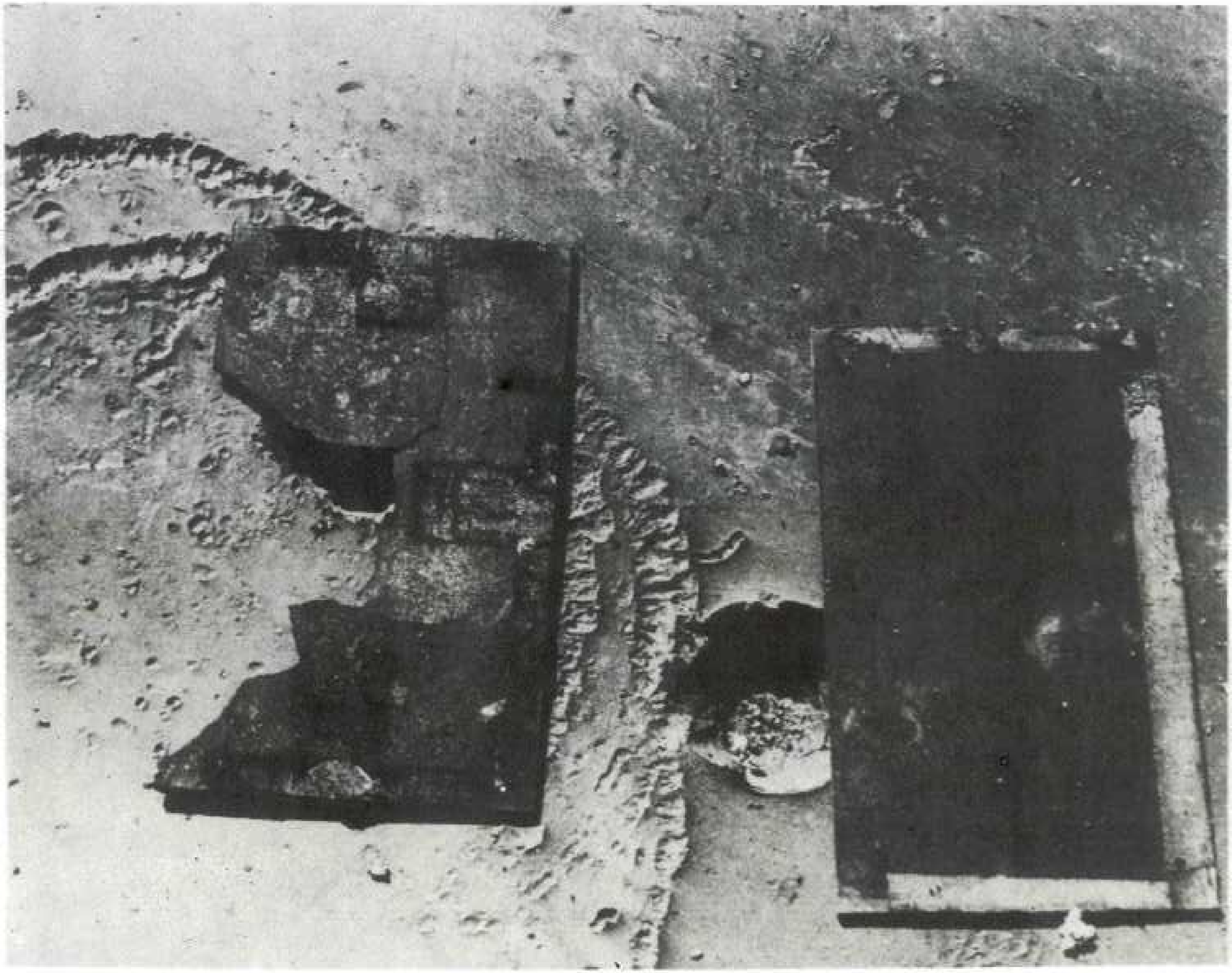

Figure 30. Cracking and Shattering of Acceptor Bucket from Blast Pressures

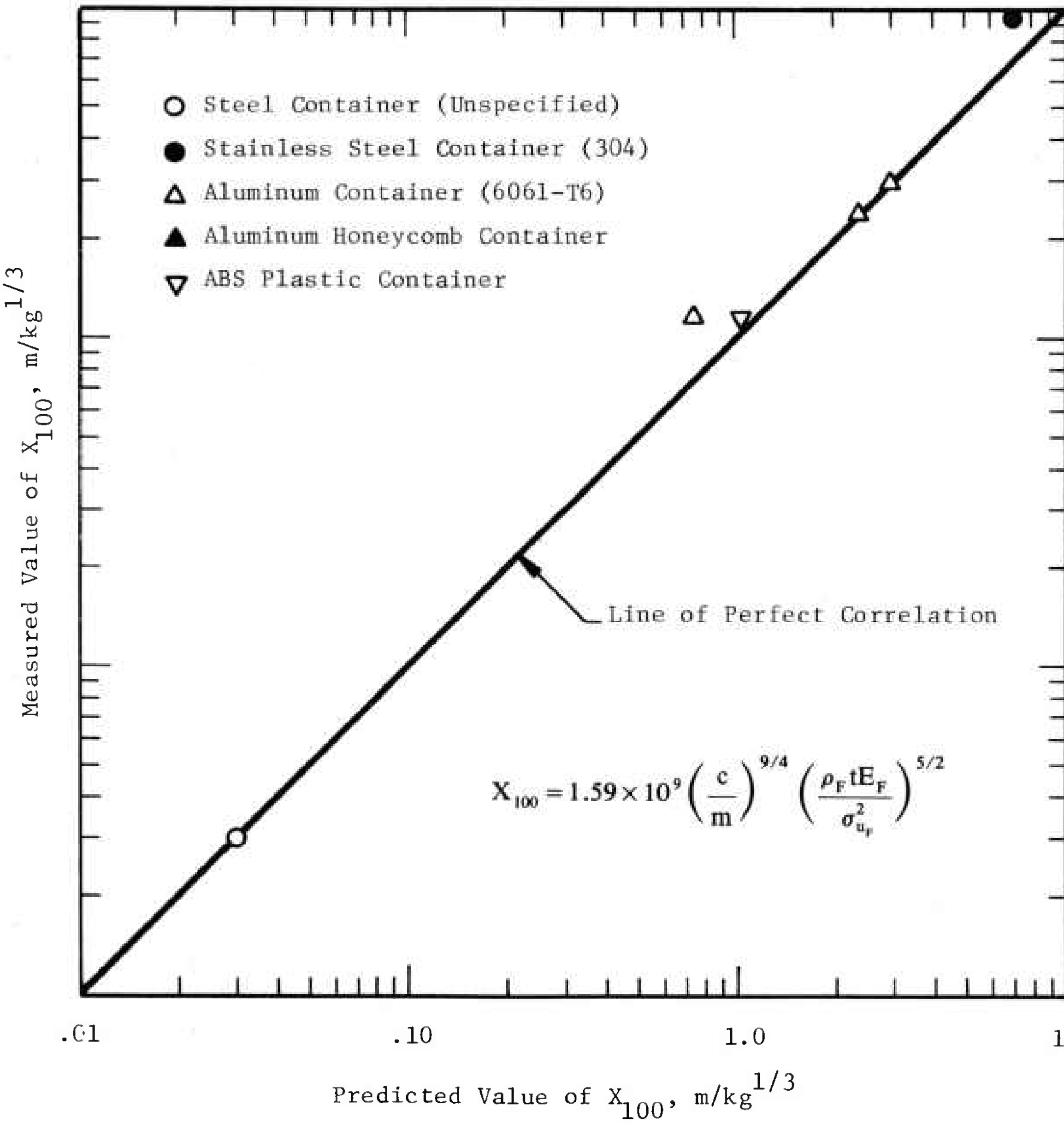

Figure 31. Safe Separation Model Form A

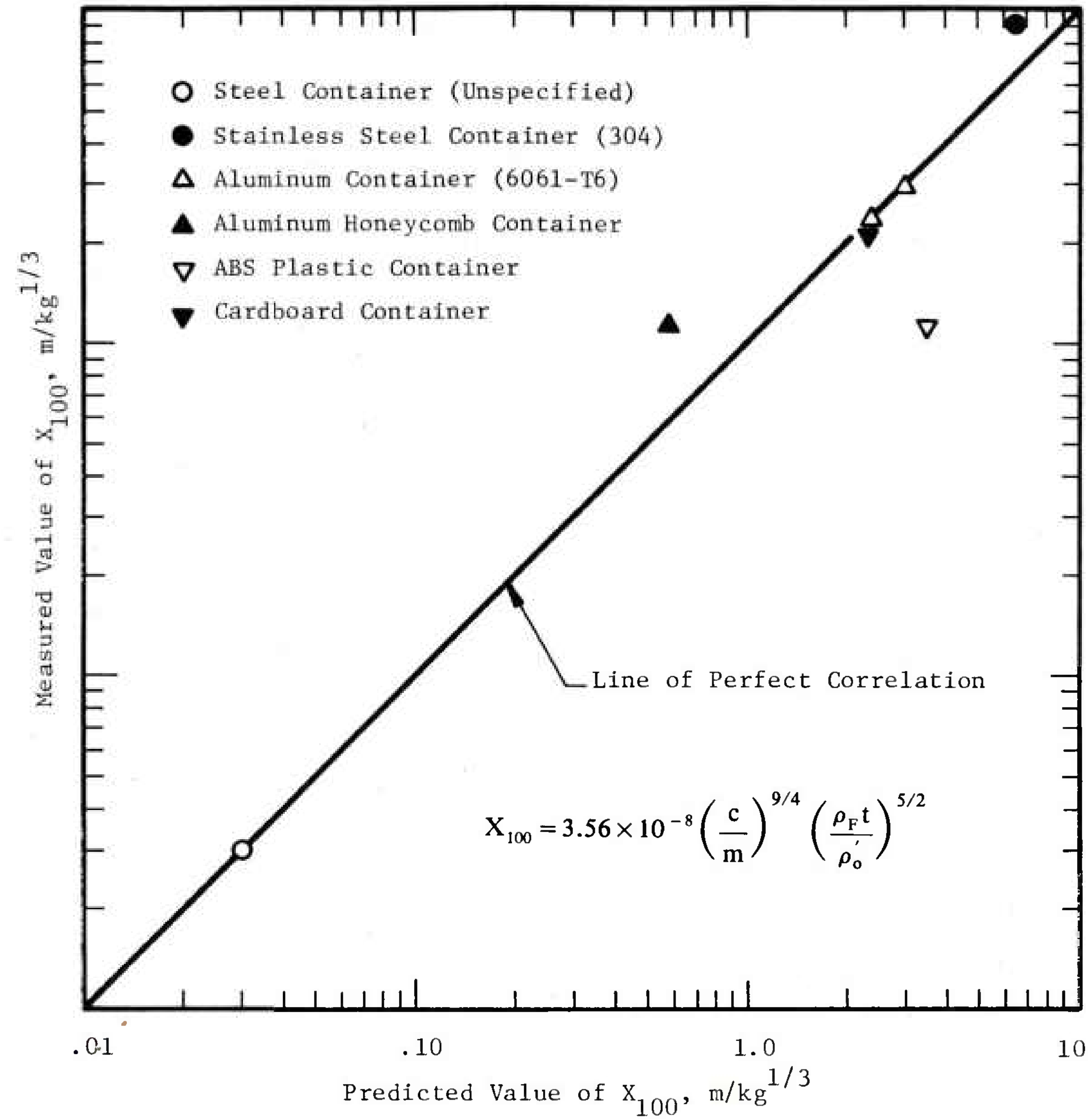

Figure 32. Safe Separation Model Form B

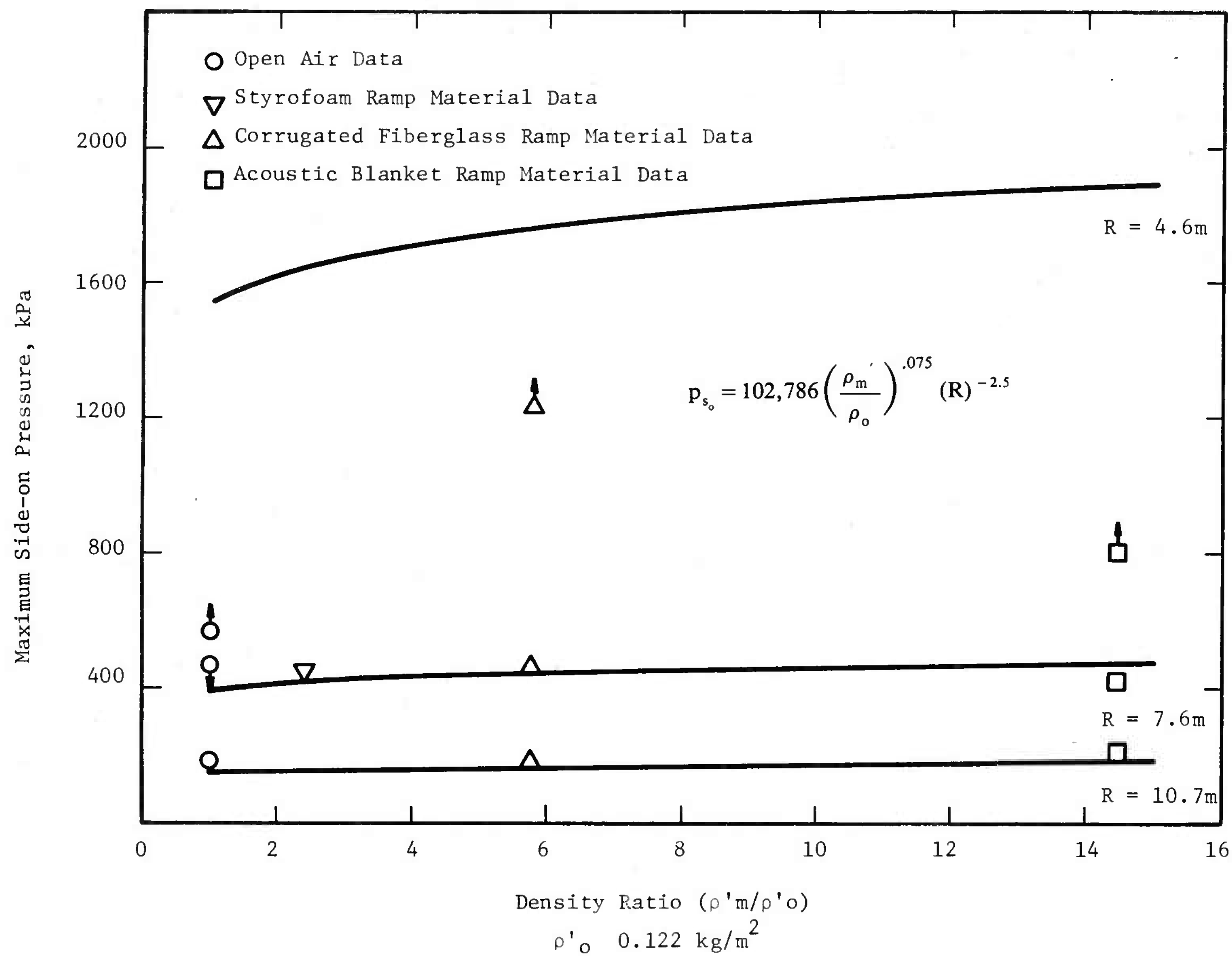

Figure 33. Peak Side-on Pressure Versus Density Ratio

DISTRIBUTION LIST

Commander
U.S. Army Armament Research and
Development Command
ATTN: DRDAR-CG
DRDAR-LC
DRDAR-LCM
DRDAR-LCM-S (12)
DRDAR-SF
DRDAR-TSS (5)
DRDAR-LCU-P
Dover, NJ 07801

Commander
U.S. Army Materiel Development and
Readiness Command
ATTN: DRCDE
DRCIS-E
DRCPA-E
DRCPP-I
DRCDI
DRCSG-S
5001 Eisenhower Avenue
Alexandria, VA 22333

Commander
USDRC Installations and
Services Agency
ATTN: DRCIS-RI-IU
DRCIS-RI-IC
Rock Island, IL 61299

Commander
U.S. Army Armament Materiel
Readiness Command
ATTN: DRSAR-IR (2)
DRSAR-IRC
DRSAR-ISE (2)
DRSAR-IRC-E
DRSAR-PDM
DRSAR-LC (2)
DRSAR-LEP-L
DRSAR-ASF (2)
DRSAR-SF (3)
Rock Island, IL 61299

Chairman
Dept of Defense Explosives Safety Board
Hoffman Bldg 1, Room 856C
2461 Eisenhower Avenue
Alexandria, VA 22331

Commander
U.S. Army Munitions Production
  Base Modernization Agency
ATTN: SARPM-PBM-EP (2)
      SARPM-PBM-LA
      SARPM-PBM-T-SF
Dover, NJ 07801

Director
Ballistics Research Laboratory
U.S. Army Armament Research and
  Development Command
ATTN: DRDAR-BLE (C. Kingery) (2)
Aberdeen Proving Ground, MD 21005

Administrator
Defense Technical Information Center
ATTN: Accessions Division (12)
Cameron Station
Alexandria, VA 22314

Commander
U.S. Army Construction Engineering
  Research Laboratory
ATTN: DERL-ER
Champaign, IL 61820

Office, Chief of Engineers
ATTN: DAEN-MCZ-E
Washington, DC 20314

U.S. Army Engineer District, Huntsville
ATTN: Construction Division-HAD-ED (2)
PO Box 1600 West Station
Huntsville, AL 35807

Commander
Indiana Army Ammunition Plant
ATTN: SARIN-OR (2)
      SARIN-SF
Charlestown, IN 47111

Commander
Kansas Army Ammunition Plant
ATTN: SARKA-CE
Parsons, KS 67537

Commander
Lone Star Army Ammunition Plant
ATTN: SARLS-IE
Texarkana, TX 57701

Commander
Milan Army Ammunition Plant
ATTN: SARMI-S (2)
Milan, TN 38358

Commander
Badger Army Ammunition Plant
ATTN: SARBA (2)
Baraboo, WI 53913

Commander
Holston Army Ammunition Plant
ATTN: SARHO-E
Kingsport, TN 37662

Commander
Iowa Army Ammunition Plant
ATTN: SARIO-A
Middletown, IA 52638

Commander
Joliet Army Ammunition Plant
ATTN: SARJO-SS-E
Joliet, IL 60436

Commander
Longhorn Army Ammunition Plant
ATTN: SARLO-O
Marshall, TX 75670

Commander
Louisiana Army Ammunition Plant
ATTN: SARLA-S
Shreveport, LA 71102

Commander
Newport Army Ammunition Plant
ATTN: SARNE-S
Newport, IN 47966

Commander
Pine Bluff Arsenal
ATTN: SARPB-ETA
Pine Bluff, AR 71601

Commander
Sunflower Ammunition Plant
ATTN: SARSU-O
Lawrence, KS 66044

Commander
Volunteer Army Ammunition Plant
ATTN: SARVO-T
Chattanooga, TN 34701

Southwest Research Institute
6220 Culebra Road
ATTN: J. W. Gehring (20)
San Antonio, TX 78284

Director
Ballistics Research Laboratory
U.S. Army Armament Research and
  Development Command
ATTN: DRDAR-TSB-S
Aberdeen Proving Ground, MD 21005

Chief
Benet Weapons Laboratory, LCWSL
U.S. Army Armament Research and
  Development Command
ATTN: DRDAR-LCB-TL
Watervliet, NY 12189

Director
U.S. Army Materiel Systems
  Analysis Activity
ATTN: DRXSY-MP
Aberdeen Proving Ground, MD 21005

Commander/Director
Chemical Systems Laboratory
U.S. Army Armament Research and
  Development Command
ATTN: DRDAR-CLJ-L
      DRDAR-CLB-PA
APG, Edgewood Area, MD 21010